EEA1 is required for CD13 localization during early epithelial polarity orientation

Anne Kim

Faculty of Medicine

Division of Experimental Medicine

McGill University, Montreal

April 2022

A thesis submitted to McGill University in partial fulfillment of the requirements of the degree in Master of Science.

Abstract

Epithelial cells establish polarity by organizing into complex structures with a characteristic central lumen in normal tissues. Lumen formation requires cells to orient their polarity axis so that the apical domain faces the inside, and the basolateral domain faces the outside of epithelial structures. Disrupted polarity is found frequently in epithelial malignancies, which account for greater than 80% of human cancers, resulting in disrupted control of cellular processes including proliferation, apoptosis, and adhesion. Our lab has previously shown that the transmembrane aminopeptidase, CD13, is a key determinant of epithelial polarity orientation. CD13 localization to the apical membrane is necessary for it to couple apical protein cargo to Rab11 endosomes and to capture endosomes in a Rab35-dependent mechanism to the apical initiation site. In the context of CD13 deficiency, cells display inverted polarity as apical proteins are found to be retained on the outer cell periphery and fail to accumulate at an intercellular apical initiation site. However, the mechanism by which CD13 is directed to the apical membrane to initiate lumen formation has yet been defined. Here, we show that early endosome-associated protein, EEA1, associates with CD13 and is required for CD13 trafficking to the plasma membrane to initialize apical membrane specification. In the absence of EEA1, cells display inverted polarity and are unable to form central lumen, which phenocopies depletion of CD13. Further, we show that phosphorylation of its intracellular tyrosine (Y6) is required for CD13 to correctly localize to the plasma membrane. A non-phosphorylatable tyrosine-to-phenylalanine mutant (CD13-Y6F) CD13 becomes trapped in EEA1+ vesicles that are unable to localize to the apical membrane. Our data provides insight into the mechanism behind early CD13 localization, which is fundamentally necessary to understand apical-basal polarity formation in epithelial cells.

Résumé

Les cellules épithéliales établissent la polarité en s'organisant en structures complexes avec des lumens centraux typiques dans les tissus normaux. La formation des lumens exige que les cellules orientent leurs axes de polarité pour que les domaines apicaux font face à l'intérieur et les domaines basolatéraux à l'extérieur des structures épithéliales. La perturbation de la polarité qui se retrouve fréquemment dans les tumeurs malignes épithéliales, représentant plus de 80% des cancers humains, résulte par la perturbation du contrôle des processus cellulaires, particulièrement la prolifération, l'apoptose et l'adhésion. La groupe McCaffrey a déjà démontré que l'aminopeptidase transmembranaire, CD13, est cruciale pour l'orientation de la polarité épithéliale. La localisation de CD13 sur la membrane apicale est nécessaire pour coupler les protéines apicales cargos aux endosomes Rab-11 et pour capturer les endosomes dans un mécanisme dépendant de Rab-35 au site de l'initiation apical. Dans le contexte d'une déficience en CD13, les cellules démontrent une polarité inversée car les protéines apicales sont retenues à la périphérie externe des cellules et ne s'accumulent pas aux sites d'initiations apicaux intercellulaires. Cependant, le mécanisme par lequel CD13 est dirigé vers la membrane apicale pour initier la formation du lumen n'a pas été encore défini. Ici, nous démontrons que la protéine associée à l'endosome, EEA1, se lie au CD13 et est nécessaire à orienter CD13 pour initier la spécification de la membrane apicale. En l'absence d'EEA1, les cellules qui affichent une polarité inversée, sont incapables de former les lumens centraux et de plus, agissent comme phénocopies de cellules pauvres en CD13. Nous montrons aussi que la phosphorylation de la tyrosine intracellulaire (Y6) est nécessaire pour localiser correctement CD13 aux membranes apicales. Une perte de phosphorylation par une mutation CD13-Y6F piège CD13 dans les vésicules EEA1 + et est incapable de se localiser sur la membrane apicale. Nos résultats suggèrent un nouveau mécanisme qui améliore notre

compréhension sur la localisation de CD13 aux premières étapes de l'initiation des membranes apicaux, qui est fondamentale pour comprendre la formation de la polarité apicale-basale dans les cellules épithéliales.

Acknowledgements

I would like to first thank my supervisor, Dr. Luke McCaffrey, for his unwavering support and guidance throughout my graduate studies for the past two years. In addition to his expertise and enthusiasm for research, his dedication to his students, shown through his genuine curiosity in our projects and his constant support in our research endeavors, makes him an incredible supervisor and mentor. By creating a great balance of guiding students in the right direction while allowing students to thrive independently, he has created a supportive network that challenges students to be creative yet critical, helping us to achieve our full potentials as researchers. I am so grateful for his mentorship, and the lessons I've learned from the lab are ones I will apply moving forward to my future career.

I would also like to thank all of the members of the McCaffrey lab that have supported me during my studies and have made the lab environment incredibly enjoyable: Dr. Li-Ting Wang, Dr. Carlis Rejon, Rachel Catterall, Mara Whitford, Dr. Élise Di Lena, Maia Al-Masri, Marie-Ève Proulx, Kassandra Blais-Vaillancourt, Christina Boghdady, Rachel Kim, James Meterissian, Gloria Ma, and Lois Lau. Specifically, I'd like to thank Dr. Li-Ting Wang for her guidance and encouragement from the beginning of my graduate studies and providing the inspiration for my project. I'd also like to thank Rachel Catterall for being an incredible knowledge source on apical-basal polarity, Marie-Ève Proulx for helping me with various experiments, and Rachel Kim for reviewing my thesis.

Finally, I'd like to thank my family and friends who have encouraged me to be where I am today. To my parents, thank you for allowing me to pursue this education and shaping me to be who I am today. To my sister, Esther, thank you for always supporting me and being willing to

listen to my presentations even though you may not understand most of the science lingo. Last but not least, I would like to thank my partner, Daniel, for being a huge source of motivation and encouragement.

Contribution of Authors

All the work presented in this thesis is my original research. It was conceived, designed, performed, and analyzed by myself, supervised by Dr. Luke McCaffrey. Dr. Li-Ting Wang sub-cloned DNA constructs used in this thesis.

Table of Contents

List of Figures

1. General Introduction and Literature Review

1.1 Epithelium Organization and Polarity

1.1.1 Epithelial Structure and Function

Epithelial cells expand during embryogenesis to form self-organized structures, including stratified sheets, alveoli, ducts or tubes, that line major organ surfaces. They serve as building blocks for tissues and organs that function together to generate a barrier between the tissue and the external environment (Macara et al., 2014). A key property of epithelial cells is that they establish plasma membrane polarity along the apical-basal axis to ensure that the apical membrane faces a central lumen that constitutes the external environment and a basolateral membrane faces the basement membrane and adjacent cells (Chatterjee & McCaffrey, 2014). Furthermore, at the level of cell-cell contact and in tissues, epithelial cells display planar polarity in which cells are organized along a polarity axis in the plane of the tissue through dynamic trafficking and feedback interactions, influencing protein stability and localization (Butler & Wallingford, 2017). Polarized epithelial cells create a barrier for selective transport of macromolecules for absorption or secretion, and also spatially regulate various signaling pathways for diverse cellular properties such as stem cell renewal, differentiation, survival, proliferation, metabolism, motility, and adhesion (Nelson et al., 2013; Rodriguez-Boulan & Macara, 2014; Roignot et al., 2013).

1.1.2 Epithelial Homeostasis

The dynamic maintenance of epithelial tissues depends on the spatial organization of signaling pathways within cells that balances epithelial cell proliferation, and apoptosis, which is necessary to maintain tissue architecture and function (Chatterjee et al., 2016). In multicellular organisms, the Yes-associated protein (YAP) transcription co-activator is essential for maintaining

organ size homeostasis by promoting proliferation and inhibiting apoptosis by targeting specific transcription factors (Zhao et al., 2011). The Hippo pathway inhibits YAP to avoid overproliferation, which is a common feature of tumorigenesis. First discovered in *Drosophila*, there are four proteins that make up the core components of the Hippo pathway. Mst1/2 kinase and scaffolding protein Sav1 first complex together to phosphorylate and activate Lats1/2 kinase. Mob1, another scaffolding protein, also acts to activate Lats1/2 kinase. The activated Lats1/2 kinase directly phosphorylates and inactivates YAP (Zhao et al., 2010). Our lab has previously linked the Hippo pathway to aPKC of the Par complex, which is essential in maintenance of apical membrane identity in epithelial cells. Specifically, gain of function of aPKC resulted in epithelial transformation as incorrect apical-basal polarity orientation in cells prevented lumen formation. Furthermore, aPKC was demonstrated to associate with Mst1/2, thereby uncoupling it from Lats1/2 kinase. As a result, inactivated Lats1/2 kinase was unable to phosphorylate YAP, promoting nuclear accumulation of YAP and overproliferation of transformed cells (Archibald et al., 2015). Others have extended such studies looking at the Hippo signalling pathway in the context of polarity complexes by demonstrating that loss of adherens junctions and manipulation of Scribble of the Scribs complex, necessary for basolateral membrane identity, resulted in upregulation of Hippo target genes, thereby hyperactivating YAP, and relied on Yorkie, a transcriptional factor downstream of the Hippo pathway, to coactivate the overproliferation process (Chen et al., 2010).

Apoptosis, a mechanism designed for programmed cell death, follows two principle signaling pathways. The first follows a more direct pathway that begins with ligation to a death receptor, which then acts to recruit the precursor form of caspase-8 to the death-inducing complex through adaptor protein Fas-associating protein with death domain (FADD). This activates

caspase-8, which acts as an initiator to activate other effector caspases, such as caspase-3. The second pathway is triggered by stimuli such as drugs, radiation, infectious agents, and reactive oxygen species, which results in cytochrome C to be released from the mitochondria and bind to Apoptotic Peptidase Activating Factor 1 (Apaf1) and ATP. This further promotes activation of caspase-9, which also acts similarly to caspase-8 to act as an initiator to activate effector caspases (Kroemer & Reed, 2000; Kuwano, 2007).

1.1.3 Apical Basal Polarity

Normal epithelial cells require proper localization of apical and basolateral domains. These domains are effectively modulated by cell-cell adhesions, which include adherens junctions, desmosomes, and apicolateral tight junctions (Chatterjee et al., 2016). Adherens junctions are composed of E-cadherin, α-catenin, and β-catenin (Elsum et al., 2012), whereas tight junctions contain transmembrane proteins, such as occludins, claudins, and junction adhesion molecule-A, as well as intracellular adaptor proteins, such as zonula occludins (ZO1-3), that aide the linking of transmembrane proteins to the cytoskeleton (Van Itallie & Anderson, 2014). Proper positioning of these complexes is necessary to establish a proper polarity axis. Epithelial cells with distinguished apical and basolateral domains are able to display proper cell-to-cell contact and communication, which ultimately establishes coherent epithelial tissue growth and maintenance (Elsum et al., 2012).

Within epithelial cells, establishing and maintaining apical-basal polarity relies on three highly conserved polarity complexes: the Scribble complex (Scrib), Crumbs complex (Crb), and ‘partitioning defective’ Par complex, of which the first two complexes were originally identified in *Drosophila melanogaster* and the last complex in *Caenorhabditis elegans* (Chatterjee et al., 2016; Elsum et al., 2012). The Scribble complex, which regulates the basolateral identity of

epithelial cells, is composed of Scribble (Scrib), discs large (Dlg), and lethal giant larvae (Lgl) (Elsum et al., 2012). In *Drosophila*, this complex is localized to the cortex basally to the adherens junction, whereas in mammalian epithelial cells, Scrib and Dlg co-localize to the adherens junction, extend basally, and overlap with Lgl (Bilder et al., 2000; Elsum et al., 2012). The activity of all three genes leads to cortical localization of Lgl and junctional localization of Scrib and Dlg (Bilder et al., 2000). Defining the apical identity of epithelial cells, there are the Crb complex, which is composed of transmembrane protein Crumbs3 (Crb3), scaffold Protein Associated with Lin7 1 (Pals1), and Pals1-associated tight junction protein (PatJ), and the Par complex, which contains scaffolding protein Par3, adaptor protein Par6, atypical Protein Kinase C (aPKC), and cell division control protein Cdc42 (Chen & Zhang, 2013; Pocha & Knust, 2013). Initially, Par3 localizes to tight junctions to recruit Par6 and aPKC (Bilder, 2003; Hirose et al., 2002). Par6 possesses a PDZ domain that binds Par3, which has a PB1 domain to form heterodimeric PB1-PB1 interactions with aPKC and a semi-CRIB domain that binds Cdc42, which acts as a GTPase to activate aPKC (Noda et al., 2001). Localization of Lgl depends on its phosphorylation by aPKC, demonstrating a mutually antagonistic relationship with aPKC. When Lgl is phosphorylated, it is unable to localize to the cortex and remains inactive; this process is evolutionarily conserved (Yamanaka & Ohno, 2008). The Crbs complex also acts antagonistically to the Scrib complex, although the precise regulatory pathway is unknown (Bilder et al., 2003; Chalmers et al., 2005). The localization and distinct identity of each polarity complex allows regulation of apical-basal cell polarity (Elsum et al., 2012) (Figure 1.1.3A).

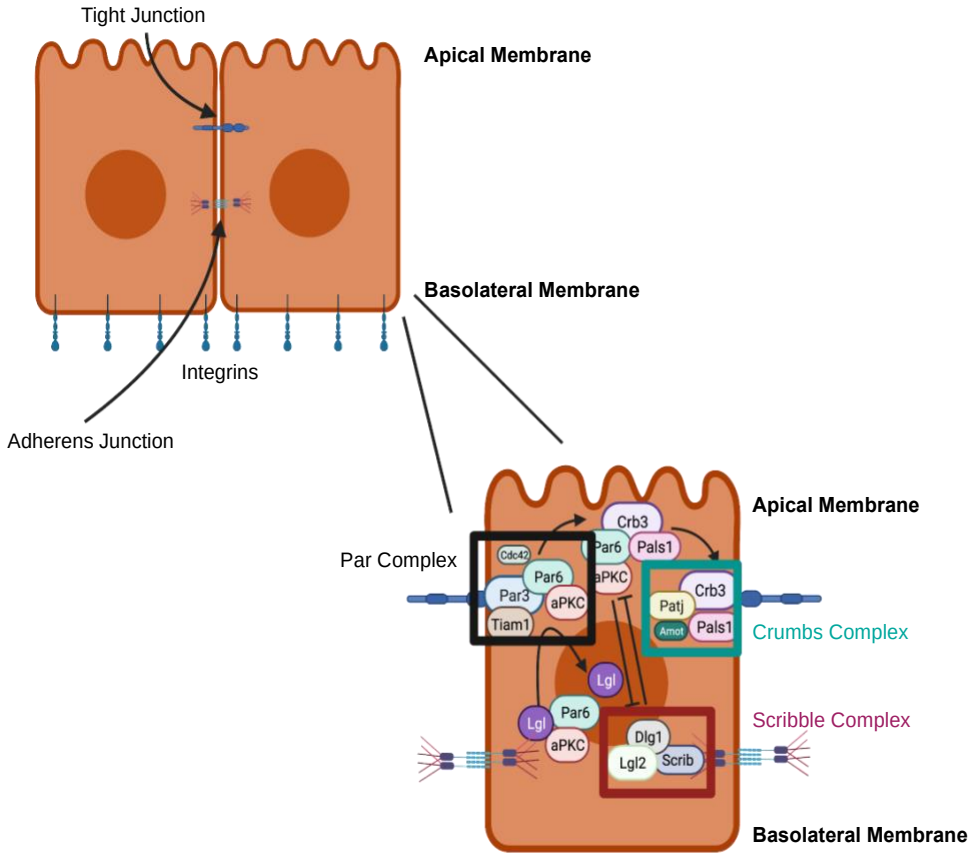

Figure 1.1.3A Apical-basal polarity complexes in epithelial cells. Apical and basolateral membrane identities of epithelial cells are developed and maintained as a result of three complexes. Proteins in the Par complex (within black box) and Crumbs complex (within green box) are necessary in maintenance of the apical membrane, and proteins in the Scribble complex (within burgundy box) are necessary in maintenance of the basolateral membrane. Illustration was modeled after on Biorender.

1.1.3.1 Three-Dimensional (3D) Cultures

A well-established model to study apical-basal polarity and *de novo* lumen formation has been the 3D tissue culturing of epithelial cells in basement membrane extract rich in laminin. Unlike two-dimensional (2D) cultures that feature cells being attached and grown in flat dishes as monolayers, the 3D culture more closely resembles the *in vivo* environment by permitting more complex contacts between cells themselves or cells and the microenvironment. Specifically, cells such as Madin-Darby canine kidney (MDCK) and Caucasian colon adenocarcinoma (Caco-2) are able to generate cysts that establish apical-basal polarity that feature a single layer of polarized cells surrounding a prominent hollow lumen (Caplan et al., 1987; Jewett & Prekeris, 2018; Pollack et al., 1998) 2018; Pollack et al., 1998). 3D cultured cells display greater viability, more resistance to drug therapies, and lower stiffness, and different proliferation rates as those cultured in 2D (Edmondson et al., 2014; Kapałczyńska et al., 2018)

1.1.3.2 Lumenogenesis

The epithelial plasma membrane is composed of an apical surface that faces a lumen and a basolateral surface that contacts adjacent cells and the extracellular matrix; therefore, after epithelial cells gain proper apical-basal polarity and form junctional complexes, they subsequently form central lumen. Cell polarity is required for lumenogenesis, which is the process by which space is created between cells to form hollow cavities (Martin-Belmonte & Mostov, 2008). There are two major mechanisms that govern lumen formation. Budding, the first mechanism, uses pre-existing polarized cellular sheets and tubes to form lumen. By permitting cells to invaginate through apical constriction, therefore entrapping central lumen from apical spaces, they form branches that subsequently extend through cell migration and division. The second mechanism is *de novo* lumen formation where epithelial structures create lumen without any pre-existing polarity

structures. This process occurs through two different processes: cavitation or hollowing. Cavitation programs central cells to undergo apoptosis, a programmed cell death mechanism while permitting cells at the periphery that contact the basement membrane to be protected from the apoptotic pathway and further polarize. Hollowing features nascent apical lumen formation through exocytosis and plasma membrane separation. Hollowing can occur by forming and expanding a lumen within one cell or by forming and expanding lumen extracellularly to share the lumen with multiple neighboring cells. Another form of *de novo* lumen formation is apicalization in which cell-cell contact is converted to a free membrane surface to expand and form lumen (Jewett & Prekeris, 2018).

1.1.3.3 Polarization Steps in Apicalization

In the context of polarity, the plasma membranes of single cells display a co-distribution of apical and basolateral proteins. One of the best models to understand establishment of polarity is seeding single epithelial cells in 3D culture and assessing localization of various polarity structures through early timepoints of division and growth as they develop into polarized multi-cellular structures that generate a hollow lumen (Figure 1.1.3B). The division of single cells into identical daughter cells or mitosis, an essential process for all living organisms, serves as the basis for lumen formation via apicalization. In the final step of cell division in the mitotic pathway, cytokinesis, cells develop a cleavage furrow, which is driven by the interaction of an actomyosin contractile ring with the plasma membrane (Frémont & Echard, 2018). Actin filaments (F-actin) and myosin-II constrict the cytokinetic furrow, and this further generates a narrow, intercellular, cytoplasmic bridge filled with microtubule bundles that connect the two daughter cells (Skop et al., 2004). This bridge eventually undergoes abscission, a process by which this bridge is severed (Mierzwa & Gerlich, 2014).

After the mitosis, the midbody, a microtubule-rich structure that is formed during cell division, recruits apical proteins to the cell-cell junction by trafficking along the midbody microtubules, generating an apical membrane initiation site (AMIS) (Frémont & Echard, 2018). After this site is defined, apical trafficking largely depends on the Rab family of small monomeric GTPases that mediate endocytosis of apical membrane proteins from the cell periphery deliver them to the forming apical domain at the midbody (Bhartur et al., 2000; J. E. Casanova et al., 1999; Goldenring et al., 1996; Wang et al., 2021). Following this, the AMIS matures into a pre-luminal apical patch (PAP) by further recruiting apical proteins that act to exclude basolateral determinants. The PAP is characterized by spatial separation of tight junctions and presence of cingulin and ZO-1 (Bryant et al., 2010; Ferrari et al., 2008). The tight junctions help create a boundary to maintain apical and basal membrane domains, and a permeability barrier so that aquaporins can generate further hydrostatic pressure to help drive lumen opening (Ferrari et al., 2008). In summary, polarized vesicle exocytosis, hydrostatic pressure, and contractile forces help establish nascent central lumen formation, establishing apical-basal polarity. The apical luminal space expands with subsequent cell divisions that maintain the apical-basal axis (Jewett & Prekeris, 2018).

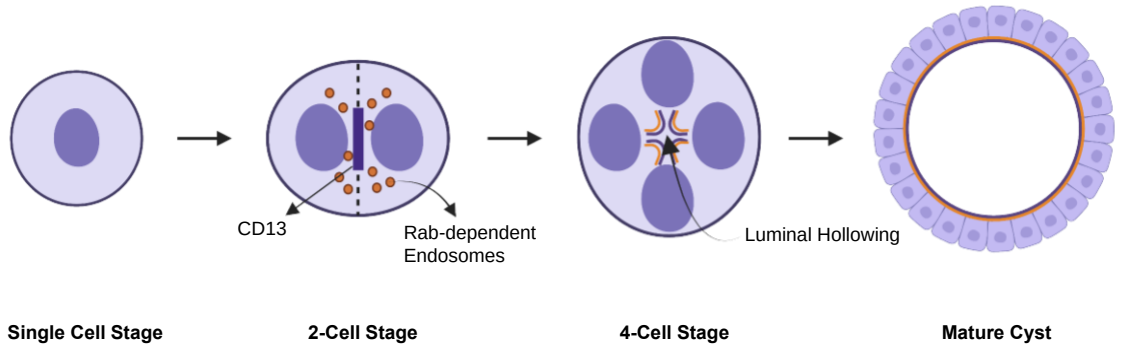

Figure 1.1.3B Stepwise progression of lumen formation in normal epithelial cells. Single epithelial cells undergrow continuous growth and cell division as they develop into mature cysts. As single cells enter the 2-cell stage, CD13 accumulates at the AMIS site and subsequently recruits Rab-dependent endosomes that mediate apical protein localization to this site. At the 4-cell stage, the nuclei arrange themselves circularly along the periphery of the plasma membrane, and CD13 and recruited apical proteins are arranged around the central point in which cells will undergo luminal hollowing. Mature cysts form prominent lumen in which the apical membrane is defined and found at the inner cell periphery. Illustration was modeled after (Catterall et al., 2020; Wang et al., 2021) on Biorender.

1.1.4 Polarity in Disease

The establishment of apical-basal polarity in epithelia is essential for integrity and function of tissues and organs (Wilson, 1997). The presence of genetic or acquired defects in polarity can result in disease pathophysiological states (Wilson, 2011). In the mammalian kidney, proper polarization of epithelia that line renal tubules are essential for the unidirectional vectorial transport of ions and fluids. Reabsorption and secretion depend on insertion of specific transporters and proteins in the apical membrane that line the renal tube lumen and basolateral membrane that neighbours the interstitium and blood space. In the proximal tubule, for example, the apical membrane of the proximal tubule contains sodium-coupled transporters implicated in reabsorption through uptake of glucose and amino acids, amiloride-sensitive sodium/hydrogen (Na/H) exchangers, and brush border proteolytic enzymes. The basolateral membrane contains sodium-potassium-adenosinetriphosphatase (Na^+/K^+-ATPase), which acts as an electrogenic sodium pump to actively transport sodium ions out of the cell to establish ion gradients for osmotic reabsorption (Wilson, 1997). Autosomal dominant polycystic kidney disease (ADPKD) is a genetic disorder in which Na^+/K^+-ATPase and epidermal growth factor (EGFR) are missorted from basolateral to apical membrane and $Na^+/K^+/2Cl^-$ cotransporter (NKCC1) is missorted from apical to basolateral membrane (Wilson, 2011; Wilson et al., 1991). Affecting 1 in 800 individuals, patients with ADPKD develop large, fluid-filled cysts in the kidneys, and in certain cases, in the liver, which lead to loss of renal function, kidney failure, and death. A mutation in poycystin-1, a protein implicated in signaling and adhesion, has been discovered in 85% of ADPKD cases (Stein et al., 2002). Localization of polycystin-1 to the adherens junctions and focal adhesions in the kidney is necessary to maintain proper renal epithelial polarity, and given that the C-terminal cytoplasmic domain of polycystin-1 stabilizes endogenous beta-catenin while stimulating TCF-dependent gene

transcription in human embryonic kidney cells, studies suggest a close relationship between polycystin-1 to the Wnt signaling pathway (Kim et al., 1999; Stein et al., 2002). Another system impacted by cell polarity is the intestinal epithelium, which depends on distinct apical and basolateral plasma membrane domains to provide barrier formation and uptake and transport of nutrients. Microvillus inclusion disease (MVID) is a disease in which the intestinal epithelial cell polarity is disrupted, resulting in symptoms like extremely watery diarrhea, dehydration, and weight loss (Schneeberger et al., 2018). MVID is found in infancy as early-onset MVID, which usually occurs within the first week of life, whereas late-onset MVID occurs within the first 3 months of life (Müller et al., 2008; Schneeberger et al., 2018). Studies have shown that MVID can be caused by mutations in *MYO5B*, a type Vb myosin motor protein, or *STX3*, an apical receptor implicated in membrane fusion of apical vesicles in enterocytes (Müller et al., 2008; Wiegerinck et al., 2014). Both proteins function as a part of the intracellular trafficking machinery within epithelial cells (Schneeberger et al., 2018). In normal conditions, MYO5B interacts with Rab11a and Rab8 proteins, which are part of various recycling systems, to regulate intracellular protein trafficking (Roland et al., 2007). With Rab8 being responsible for proper localization of apical proteins in intestinal epithelial cells in mice, in its absence, apical peptidases and transporters seem to mislocalize to lysosomes in the small intestines. The phenotype of Rab8 deficiency closely resembles the effects of MVID, suggesting its relationship plays a role in the manifestation of the disease (Sato et al., 2007). *STX3*, which is less frequently mutated in MVID patients, acts as an apically targeted soluble N-ethylaleimide-sensitive factor attachment protein receptor (SNARE) to establish and maintain polarity by assembling into complexes with vesicular SNARE proteins, which are then attached to recycling vesicles (Delgrossi et al., 1997; Jahn & Scheller, 2006;

Sharma et al., 2006). Disrupted STX3 function impaired delivery of apical markers *in vitro,* adding to the literature that disrupted apical-basal polarity promotes disease (Wiegerinck et al., 2014).

Epithelial malignancies can arise when cells display a loss of growth control, altered tissue organization, and loss of cell polarity. Specifically, disrupted cell polarity has been determined to be frequent in epithelial malignancies, found in 86% of human cancers, which are called carcinomas (Halaoui & McCaffrey, 2015). Disrupted apical-basal polarity as a result of alterations to polarity genes is frequently observed in many carcinomas (Bostwick & Cheng, 2012; Elsum & Humbert, 2013; Kamangar et al., 2006; Siziopikou, 2013; Zhan et al., 2008). All core polarity genes from the three polarity complexes have been implicated in carcinogenesis; interestingly, although apical-basal polarity itself is considered a tumor suppressive property, individual polarity proteins have been described to have both tumour suppressive and promoting roles depending on the context (Huang & Muthuswamy, 2010). Epithelial malignancies are prominent in cancers such as breast cancer, which is a leading cause of cancer-related deaths worldwide in women (Kamangar et al., 2006). Although the research conducted over the past two decades have led to considerable progress in understanding the disease, specifically in the diagnoses and treatments, its high heterogeneity at the molecular and cellular level leave unresolved clinical and scientific problems (Perou et al., 2000; Sørlie et al., 2001). For example, a current unresolved controversy is based on the explanations behind tumour heterogeneity. One explanation, the cancer stem cell hypothesis, stipulates that differentiated cancer cells arise from cancer stem cells rather than cells that have undergone self-renewing cell division. As a result, only the cancer stem cells are subject to genetic changes that drive tumour progression and drug resistance. Another explanation is the clonal evolution model, which postulates that a combination of properties, including the cell type of the tumor-initiating cells, genetic and epigenetic alterations, and surrounding paracrine signals, drive

the changes in various tumour cell phenotypes. These cells have the capacity to undergo self-renewing division, and all contribute to tumour progression and drug resistance (Polyak, 2007).

Breast cancer is composed of two main histological types: ductal carcinomas, in which cancer originates from cells in the mammary ducts and accounts for majority of breast cancer cases at 85-90%, and lobular carcinomas, which arises from lobules that supply the ducts with milk (Dossus & Benusiglio, 2015; Sharma et al., 2010). Specifically, ductal breast cancers progress through a series of stages. Flat epithelial atypia (FEA) and atypical ductal hyperplasia (ADH) are benign lesions. FEA lesions are composed of dilated ducts lined with one or more layers of epithelial cells, whereas ADH are made up of disorganized multilayered ducts that possess several cells lacking apical-basal polarity. These lesions predispose patients to development of ductal carcinoma in situ (DCIS), which is characterized by its loss of ductal lumen and proliferation of non-polarized malignant cells. As the myoepithelial layer is lost and cells begin to breach the basement membrane, the cancer progresses towards an even more malignant phenotype called invasive ductal carcinoma (IDC) (Rejon et al., 2016). Our lab recently demonstrated that genetic amplification and alterations to epithelial polarity genes, *PARD6B, PRKCI, SCRIB,* and *LLGL2* were implicated in the loss of polarity seen in epithelial cells with the progression of breast cancer. As these genes reside in chromosomal regions containing known driver oncogenes, specifically *PARD6B/SRC, PRKCI/PIK3CA, SCRIB/MYC, LLGL2/ERBB2*, these core polarity proteins likely contributed to the oncogenic potency of certain amplicons (Catterall et al., 2020). The variety of diseases that are implicated in disrupted apical-basal polarity highlights the importance of understanding the mechanisms surrounding development and maintenance of apical-basal polarity.

1.2 Involvement of CD13 in Apical-Basal Polarity

1.2.1 General Functions of CD13

Aminopeptidase N (CD13), a dimeric membrane protein, belongs to the M1 family of zinc dependent metalloproteases that are characterized by conserved HExxHx18E zinc-binding domains and GxMEN catalytic motifs. Structurally, CD13 has a short amino-terminal intracellular domain, helical transmembrane anchor, and an extracellular stalk that connects to the C-terminal catalytic ectodomain (Wong et al., 2012). The ectodomain cleaves terminal amino acids from oligopeptides in various physiological functions such as angiotensin activation, amino acid metabolism, and neuropeptide processing (Bauvois, 2004; Mina-Osorio, 2008). The N in its name gives away its affinity for neutral amino acids on unsubstituted oligopeptides, amides, or arylamides, apart from peptides that contain proline in the penultimate position (Hooper, 1994). The catalytic activity of CD13 is implicated in the enzymatic regulation of various peptides (Mina-Osorio, 2008). Playing a role in renal blood pressure regulation, renal tube CD13 decreases basolateral Na^+/K^+-ATPase, which are preeminent Na^+ transporters in renal tubule epithelial cells, affecting the regulation of Na^+ flux (Kotlo et al., 2007). CD13 also hydrolyzes the N-terminal arginine in angiotensin III to generate angiotensin IV (Ang IV), which promotes natriuresis (Hamilton et al., 2001; Kotlo et al., 2007). In kidneys, the primary Ang IV receptors are insulin-regulated membrane aminopeptidases (IRAP), which are present in proximal and distal tubules, vascular smooth muscle, and endothelial cells (Albiston et al., 2001; Hamilton et al., 2001; Handa, 2001). As Ang IV becomes activated through IRAP, they stimulate a cascade of pathways that include mitogen activated protein kinases (MAPKs), such as extracellular-signal-regulated kinase (ERK1/2), which has previously been reported as central regulators of cell proliferation, and tyrosine phosphorylation of focal adhesion kinases and paxillin, which provide signaling and

scaffolding functions (Chen et al., 2001; Danziger, 2008; Handa, 2001). The catalytic function of CD13 extends to cytokines and chemokines by processing ligands such as CXC chemokine ligand (CXCL11), which is produced by leukocytes, fibroblasts, and endothelial cells upon stimulation with interferons (IFNS) (Loos et al., 2006). CD13 generates truncated CXCL11 forms, which demonstrate reduced binding, signaling, and chemotactic properties for lymphocytes. Further processing and truncation of CXCL11 by CD13 resulted in a reduction in the inhibition of endothelial cell migration, demonstrating a loss of lymphocyte and NK-cell chemotaxis in addition to an enhanced angiogenic environment. In the context of inflammation and cancer development, CD13 impairs CXCL11 from attracting lymphocytes and NK cells to inflamed tissues and tumours and helps generate new blood vessels used for tumour growth (Proost et al., 2007).

CD13 also exhibits several functions independent of its catalytic activity, such as cell-cell adhesion in inflammatory cells, binding of cytokines, and acting as receptors for coronaviruses (Bauvois, 2004; Pasqualini et al., 2000). Specifically, in the context of cell-cell adhesion, CD13 acts independently of its enzymatic function to act as a signal regulator for other molecules, such as immunoglobulin G in human peripheral blood monocytes and anti-CD13 monoclonal antibodies to induce homotypic aggregation in promonocytic U-937 cells (Mina-Osorio & Ortega, 2004; Mina-Osorio et al., 2006). Previous studies have demonstrated that cross-linking of CD13 by antibodies results in monocytic cell activation, characterized by increased FcR-mediated phagocytosis, Ca^{2+} flux, cytokine secretion, and increased adhesive capacity of the cells, through signal transduction-dependent mechanisms (Mina-Osorio & Ortega, 2005; Mina-Osorio et al., 2006; Santos et al., 2002). The increase in adhesion to the endothelium seems to act distinct from inflammatory cytokines as this adhesion requires CD13 to cluster and combine into monocytic and endothelial complexes. In the absence of CD13, adhesion was abrogated. CD13 seems to actively

partake in the adhesive interaction based on the role of cell surface adhesion molecules to guide the adhesion and migration of circulating leukocytes across the endothelial cells that line the blood vessels to access site of injury during inflammation (Mina-Osorio et al., 2008). CD13 has also been implicated in osteoarthritis by binding to 14-3-3ε protein, a subchondral bone soluble mediator that alters cartilage homeostasis by promoting deleterious biochemical interactions between bone and cartilage (Nefla et al., 2015; Priam et al., 2013). CD13 was first identified to be present on chondrocytes, and further analysis by knocking down CD13 indicated a reduction of 14-3-3ε-induced markers of osteoarthritis, MMP-3, and MMP-13. Given this, it was proposed that CD13 acts as a direct binding receptor to 14-3-3ε protein, and it promotes signals in chondrocytes to induce catabolic phenotypes that promote progressive degradation of articular cartilage, synovial inflammation, and remodeling of subchondral bone, which are characteristics of osteoarthritis (Nefla et al., 2015). Finally, CD13 acts as a major viral receptor for coronaviruses in several species, including transmissible gastroenteritis virus (TGEV) of swine, porcine respiratory coronavirus, and feline infection peritonitis virus (Delmas et al., 1992; Delmas et al., 1994). Human CD13 acts as the cellular receptor for HCoV-229E, identified by using murine fibroblasts, which were found to only be susceptible to the virus after transfection with human CD13 expression (Yeager et al., 1992). In addition, human CD13 is implicated infection by additional viruses such as cytomegalovirus since it incorporates CD13 into its envelope (Larsson et al., 1998). Human CD13 has a high degree of similarity to porcine CD13 and feline CD13 by sharing similar sequence identity and numerous N-linked glycosylation sequons (Altschul et al., 1997; Wentworth & Holmes, 2001).

1.2.2 Effect of CD13 on Polarity

Given the variety of non-catalytic functions that CD13 possesses, it was of interest to examine a role for CD13 in epithelial polarity. Our lab recently demonstrated that CD13 is a necessary component of the endocytic machinery that controls apical membrane specification and lumen formation in Caco-2 cysts. Specifically, in early polarization steps, CD13 simultaneously carries out two functions. First, CD13 associates with the apical Par6/Crumbs complex by coupling it to its subapical endosomal compartments for Rab-11 dependent delivery to the midbody to promote apical membrane formation. CD13 initially localizes to the newly formed cell-cell contact site and subsequently is redistributed to accumulate at the nascent AMIS. These steps are then necessary to correctly localize Rab35 to capture incoming apical recycling endosomes to expand the apical domain. CD13 has been discovered to act as an apical protein in epithelial cells by interacting with apical complex proteins such as Par6, aPKC, Pals1, and Crb3, but not Par3. In the absence of CD13, lumenogenesis is blocked as it induces an inverted polarity phenotype in Caco-2 cysts, characterized by apical complexes and tight junctions being positioned at the periphery rather than basolateral proteins. The dynamics of early polarization steps leading to lumenogenesis indicates that CD13 is necessary for proper trafficking and localization of apical proteins to form lumen structures (Wang et al., 2021). Although we now understand the role of CD13 in apical-basal polarity in epithelial cells, the mechanism by which CD13 initially localizes to the cell-cell contact site remains yet unknown.

1.2.3 Role of the intracellular domain of CD13

Looking closer at how CD13 carries out its adhesion functions, monocytic CD13 has been extensively studied to assess the mechanism by which it activates endothelial cells that are necessary for resolving damaged tissues at injury sites (Mosser, 2003; Muller, 2011; Shi & Pamer,

2011; Wiegerinck et al., 2014). While studying the tyrosine-kinase and microtubule-dependent molecular mechanisms that mediate this, CD13 was found to induce phosphorylation of a variety of proteins, including Src, FAK, and ERK on U937 monocytic cells. These kinases that are implicated in CD13 adhesion are interconnected (Castellano & Downward, 2011; Subramani et al., 2013). Src binds to FAK via the Src-SH2 domain, promoting FAK phosphorylation. This further helps generate binding sites on FAK in SH2 domains for downstream molecules such as PI3K and Rac. Rac and Raf phosphorylation promote activation of the ERK pathway (Chuderland & Seger, 2005). Together, Ras and Src are also implicated in induction of calcium fluxes, which as previously mentioned, are characteristic of monocytic cell activation upon CD13 induction (Choi et al., 2005; Rausch et al., 1990; Rosado et al., 2000). The cytoplasmic tail of CD13, composed of 7 amino acids, was initially thought to be inert, but a previous study looking into tyrosine phosphorylation of CD13 indicates that its tyrosine 6 (Y6) residue is phosphorylated in a Src-dependent manner (Subramani et al., 2013). Y6 phosphorylation is interesting because its short cytoplasmic tail was originally thought to be too small to have any meaningful interactions with the cytoskeleton (Shipp & Look, 1993). CD13 seems to become phosphorylated by a Src protein tyrosine kinase, which in normal conditions, is activated as a result of stimulation of cell surface receptors like tyrosine kinase and integrin receptors or by cellular stress (Okutani et al., 2006; Subramani et al., 2013). Due to its interaction with a variety of proteins implicated in signal transduction and cellular function, Src protein tyrosine kinase is involved in various cell regulation processes, such as proliferation, differentiation, survival, and metabolism (Okutani et al., 2006). Mutation of this conserved cytoplasmic residue tyrosine to phenylalanine altered the cytoskeleton, and abrogated cell adhesion, and phosphorylation of SRC, FAK, and ERK (Subramani et al., 2013). Tyrosine phosphorylation of surface proteins upon crosslinking of cell surface molecules,

such as CD13, is indicative of the early stages in activation of leukocytes during inflammation (Buono et al., 2011; Hegen et al., 1997). Given the downstream activation of Src, FAK, and ERK intracellular signaling proteins by CD13, which all have well-established roles in inflammation, it further adds to the idea that CD13 is largely implicated in regulating inflammatory adhesion and monocyte trafficking (Subramani et al., 2013).

With this, our lab wanted to identify how Y6F may be implicated in restoring polarity orientation in CD13-depleted Caco-2 cells. Interestingly, in control cysts with endogenous CD13 that expressed CD13-Y6F, polarity was maintained, indicating that Y6F does not behave as a dominant negative protein. However, in the context of depleted endogenous CD13, overexpressed CD13-Y6F localized to intracellular puncta in both early (2-cell) and mature (>10 cell) stages, indicating that CD13-Y6F becomes locked in vesicular compartments rather than being translocated to the outer plasma membrane. CD13 also had a reduced association with Par6. The staining pattern of CD13-Y6F was reminiscent of the endoplasmic reticulum (ER); however, when the cysts were stained for calreticulin, a marker of ER involvement, CD13-Y6F was found to be only modestly retained within the ER (Wang et al., 2021). This suggested a yet unknown process by which CD13-Y6F is trapped in the vesicular compartment.

1.2.4 Involvement of CD13 in Rab11 and Rab35-mediated Apical Protein Trafficking

The early polarization steps and apical trafficking largely depends on the Rab family of small monomeric GTPases to mediate apical protein trafficking to the AMIS upon formation (Wang et al., 2021). Rab proteins belong to a family of small GTP-binding proteins that function as molecular switches as it alternates between the active GTP-bound state and the inactive GDP-bound state. There are 11 known yeast isoforms and around 60 Rab proteins within mammalian cells (Schimmöller et al., 1998). Rab GTPases reversibly associate with membranes through

hydrophobic geranylgeranyl groups that are, in most cases, attached to carboxy-terminal Cys residues. This association allows them to regulate intracellular vesicle trafficking by facilitating vectorial traffic through associations with the cytoskeleton, regulating vesicle docking through recruitment of effector molecules and forming molecular tethers, and priming the docking and fusion of vesicles by activating SNARE molecules (Gonzalez & Scheller, 1999; Novick & Zerial, 1997; Schimmöller et al., 1998; Stenmark, 2009).

Intracellular trafficking is a necessary process for cellular activities to occur such as cellular uptake, transportation of nutrients for metabolism and pathogens for degradation, and transportation of signalling molecules (Muro, 2018). The specialized pathways that are used for transportation of proteins, lipids, and solutes are called membrane trafficking pathways, and this can be divided into two basic movement pathways: endocytosis and exocytosis (Kumar et al., 2020; Watson et al., 2005). The early compartments of the endocytic pathway are composed of Rab4, Rab5, Rab17, Rab18, and Rab20 (Lutcke et al., 1994; Lütcke et al., 1993; van der Sluijs et al., 1992). Early endosomes comprise two functionally distinct compartments (Ghosh et al., 1994). First, internalized receptors and ligands enter the peripheral sorting endosome where proteins for degradation are separated from other proteins that are recycled back to the plasma membrane. Recycling to the plasma membrane can occur through the fast cycle, which features proteins being trafficked directly by the sorting endosomes, or through the slow cycle, which traffics protein through recycling endosomes (Dunn et al., 1989; Ghosh & Maxfield, 1995). Within the slow endocytic vesicle recycling pathway of intracellular trafficking, the two Rab proteins at play are Rab11 and Rab35 (Stenmark, 2009). Rab11 and Rab35 mediate the endocytosis of apical membrane proteins to deliver them to the forming apical domain (Wang et al., 2021). The Rab11 subfamily is constituted of Rab11a, Rab11b, and Rab25, and the Rab11 protein is apically located

to play a central role in transcytosis and recycling of apical proteins for lumen formation in epithelial complexes (Drivas et al., 1991; Jedd et al., 1997). Given this, our lab previously inquired whether CD13 influences Rab11-dependent vesicle trafficking during epithelial polarization, and we discovered that CD13 coalesces to the AMIS without Rab11 enrichment, indicating that CD13 localization occurs prior to Rab11 trafficking. Furthermore, CD13 was discovered to be required for proper trafficking of Rab11-mediated apical proteins (Wang et al., 2021). Rab35, another recycling endosomal protein, controls the endocytic recycling pathway by localizing to the plasma membrane and endocytic compartments. Rab35 is essential for maintaining the proper steps in the later stages of cytokinesis, specifically in the intercellular bridge localization of molecules essential for the post-furrowing steps (Kouranti et al., 2006). In the context of polarity, Rab35 acts as a receptor to capture apical protein vesicles at the AMIS, and a previous study has indicated that in the absence of Rab35, vesicles are unable to dock, resulting in apical proteins being recycled to the cell periphery and displaying inverted polarity (Klinkert et al., 2016). Having determined the involvement of CD13 for mediating Rab35, our lab discovered that CD13 also precedes Rab35 accumulation to the AMIS, and CD13 presence is necessary for apical cargo carrying endosomes to properly dock (Wang et al., 2021).

1.3 Alternate Mechanisms of Apical and Basal Protein Sorting

Apical and basolateral membrane proteins are sorted in a biosynthetic pathway, relying on specific transport carriers to deliver them to the appropriate plasma membrane domain (Drubin & Nelson, 1996; Nelson & Yeaman, 2001). Unlike basolateral targeting signals that often involve tyrosine or dileucine based motifs, there is less known about apical targeting signals (Matter & Mellman, 1994). Some apical proteins have been associated with glycolipid raft domains through their membrane-anchoring domains, and others have been shown to have N- or O-linked

oligosaccharides in their extracellular domains that interact with lectin to specify apical transport (Ikonen & Simons; Scheiffele et al., 1995). Apical targeting signals contrast basolateral signals by functioning only in the absence of these signals (Matter & Mellman, 1994).

Apical and basolateral proteins depend on the process of endocytosis to be trafficked to their proper location. Many proteins are transported in endosomes to maintain polarized distributions (Mellman, 1996). Following endocytosis, the proteins are delivered to early endosomes, and these endocytosed proteins are either able to recycle to the surface of origin, be degraded as late endosomes or lysosomes, or be transcytosed to the opposite surface (Mostov et al., 2000). Studies looking into adherens junction and tight junction proteins such as E-cadherin, occludin, and JAM-1, which are key regulators of epithelial polarity, were shown to undergo this first process of endocytosis to generate early endosomes in a clathrin-mediated process (Gonzalez-Mariscal et al., 2003; Ivanov et al., 2004; Tsukita et al., 2001). However, rather than co-localizing with markers of late and recycling endosomes, lysosomes, or Golgi, following their entrance into early endosomes, they appear to be distributed into unique storage compartments, suggesting that apical proteins may be alternatively undergoing transcytosis, a form of vesicular transport of macromolecules from one side of the cell to the other within membrane-bound carriers (Bidaud-Meynard et al., 2019; Tuma & Hubbard, 2003).

1.3.1 Transcytosis

Transcytosis is a mechanism that allows the movement of macromolecular cargo between two environments without disrupting the distinct compositions of each environment (McBride et al., 1999; Tuma & Hubbard, 2003). Vesicular transcytosis is predominantly studied in epithelial tissues, although transcytosis is a process seen in a variety of cell types, including osteoclasts and neurons (Hémar et al., 1997; Nesbitt & Horton, 1997). Transcytosis is a mechanism that has

previously been proposed as a mechanism to position apical proteins like dimeric IgA (dIgA) bound to polymeric immunoglobulin receptor (pIg-R). The dIgA-pIgR complex is transported from the basolateral surface to apical surface in epithelia (Mostov et al., 2000). The complex's initial insertion to the basolateral surface depends on a basolateral targeting signal found on the 17-amino acid sequence in its cytoplasmic tail (Aroeti et al., 1993; Casanova et al., 1991). After basolateral insertion, the complex is then internalized and transported to the apical domain (Hirt et al., 1993; Song et al., 1994). This transcytosis process is made more efficient by the serine phosphorylation of its cytoplasmic tail and by p62^{yes} src-family tyrosine kinase, although how it drives pIg-R transcytosis remains unknown (Casanova James et al., 1990; Luton et al., 1999; Mostov et al., 2000).

1.3.1.1 Endocytosis and Early Endosomes

The first process of transcytosis features molecules being endocytosed into early endosomes, and early endosome antigen 1 (EEA1) acts as a marker for the docking of incoming endocytic vesicles prior to fusion with early endosomes (Wilson et al., 2000). Internalized adherens junction and tight junction polarity proteins such as occludin, E-cadherin, B-catenin, and JAM-1 were found to co-localize with EEA1 at early stages of endocytosis, suggesting its potential implication in polarity formation (Gonzalez-Mariscal et al., 2003; Ivanov et al., 2004; Tsukita et al., 2001). In a recent study looking into the apical polarity of cystic fibrosis transmembrane conductance regulator (CFTR), basolaterally internalized CFTR relied on transcytotic endosomes, which were EEA1+, for delivery to the apical membrane (Bidaud-Meynard et al., 2019). CFTR, the anionic selective channel ABC transporter, was found to be predominantly expressed at the apical PM of secretory and resorptive epithelia to maintain ionic composition and volume homeostasis of airway surface liquid, preventing uncontrolled infection and inflammation of the lung, which are

characteristic of cystic fibrosis deaths (Bidaud-Meynard et al., 2019; Rowe et al., 2005). In the absence of transcytosis, CFTR was missorted and localized to the basolateral PM, suppressing its transepithelial anion secretion efficiency. Specifically, this decreased apical Cl^- secretion through reduction of basolateral Cl^- entry, resulting in attenuated coupled water secretion and mucociliary clearance of airway epithelia (Ballard et al., 2002; Bidaud-Meynard et al., 2019; Farmen et al., 2005). Another study looking at Madin-Darby canine kidney (MDCK) cells determined that NgCAM, a cell adhesion molecule that is apical in epithelia, was targeted to the apical surface through transcytosis in a manner similar to CFTR (Anderson et al., 2005; Walsh & Doherty, 1997). After NgCAM was determined to be an apical protein that was transcytosed from basolateral-to-apical domain in MDCK cells, it was assessed whether its cytoplasmic tail was necessary for its localization. Truncation of the NgCAM cytoplasmic tail prevented transcytosis and inhibited its ability to localize to the apical membrane. Furthermore, given that many basolateral targeting signals include critical tyrosine residues, tyrosine 33 in the cytoplasmic tail was mutated to alanine to assess its function in NgCAM in its initial delivery and endocytosis at the basolateral domain (Anderson et al., 2005; Matter et al., 1992; Schaefer et al., 2002; Tuvia et al., 1997). NgCAM was unable to insert at the basolateral domain for proper transcytosis. It was then proposed that the basolateral targeting of NgCAM may depend on phosphorylation of tyrosine by a src family kinase (Anderson et al., 2005).

EEA1 acts as an effector protein of early endosomal Rab5 protein (Wilson et al., 2000). Recent studies have shown that EEA1 interacts with the GTP-bound form of Rab5 to mediate early endosomal fusion *in vitro* (Simonsen et al., 1998). As mentioned, there are various mammalian Rab proteins that are implicated in membrane transport. Specifically, Rab1, Rab2, Rab3D, Rab4, Rab5, Rab6, and Rab11 have been implicated in regulating polarized plasma membrane transport,

and of these Rab proteins, nine localize to the apical pole. Rab3D localizes to the apical plasma membrane, Rab3B and Rab13 localize to the tight junction, and Rab5, Rab11, Rab17, Rab18, Rab20, and Rab25 all localize to subapical structures (Tuma & Hubbard, 2003). Rab5B, the most extensively studied isoform, localizes to the plasma membrane, clathrin-coated vesicles, or early endosomes. Overexpression of Rab5B has shown to increase endocytic transport and stimulate early endosome fusion *in vitro* (Christoforidis et al., 1999). Given the presence of Rab5 in early apical and basolateral endosomes in hepatocytes, hepatic WIF-B cells, mouse kidney epithelial cells, and MDCK cells, it became of interest to study Rab5 effector proteins implicated in early endosomes (Christoforidis et al., 1999; Saitoh et al., 2017; Wilson et al., 2000).

1.3.1.2 Exocysts

In the generation and maintenance of epithelial polarity, a key process is the delivery of newly synthesized and endocytosed proteins to the correct apical or basal PM domain (Yeaman et al., 1999). The exocyst, an evolutionarily conserved eight-subunit protein complex made up of Sec3, Sec5, Sec6, Sec8, Sec10, Sec15, Exo70 and Exo84, generates protein-protein interactions to tether exocytic carriers to their target membranes (Munson & Novick, 2006; Wang & Hsu, 2006). In epithelial cells, the exocyst localizes to a variety of locations such as the Golgi apparatus, the trans-Golgi network (TGN), and recycling endosomes, and is implicated in not only exocytosis and cell polarity, but also in autophagy, cytokinesis, cell migration, and tumorigenesis (Lepore et al., 2018; Wu & Guo, 2015; Yeaman et al., 2001). The exocyst complex requires all eight subunits to tether secretory vesicles, and the loss of one subunit can result in cell death or an embryonic lethal phenotype (Ahmed & Macara, 2017; Mizuno et al., 2015). The subunits exist as 2 distinct sub-complexes: subcomplex 1 is composed of Sec3, Sec5, Sec6, and Sec8, and subcomplex 2 is composed of Sec10, Sec15, Exo70, and Exo84 (Ahmed et al., 2018; Nishida-Fukuda, 2019).

Although these subcomplexes can be transported to the PM independently and associate with vesicles, they cannot trigger fusion without its partner subcomplex. Vesicle fusion is tightly controlled by the coordination of tethering complexes like the exocyst complex, GTPases, and SNARE proteins (Nishida-Fukuda, 2019). Of the various GTPases, the Rab proteins represent the largest proportion, and notably, Sec15 acts as an effector for Rab11 as the C-terminal region of Sec15 binds to Rab11a in vitro in a GTP-dependent manner (Rodriguez-Boulan & Macara, 2014; Zhang et al., 2004). In addition, Rab11 has been implicated in its association with the exocyst complex to deliver Crb to the apical surface through the Golgi and apical recycling endosomes (Roeth et al., 2009; Schlüter et al., 2009). The exocyst complex and small GTPases remain at the PM for around 10-18 seconds prior to vesicle fusion, and although the process of tethering exocyst complexes is not well known, it is likely that this is when the complex promotes assembly of SNARE proteins (Ahmed et al., 2018; Nishida-Fukuda, 2019; Rivera-Molina & Toomre, 2013). Sec3 promotes formation of the initially binary trans-SNARE complex *in vitro*. The SNARE proteins are necessary for vesicle fusion to provide the energy that is required for membrane fusion of delivered cargo (Nishida-Fukuda, 2019; Yue et al., 2017). The process of vesicle fusion features the apposition of two membranes, and this requires removal of hydration layers, local membrane bending, merging of two proximal leaflets, and the expansion of fusion pores (Witkowska et al., 2021). Prior to vesicle fusion, Sec3 leaves first, and this is subsequently followed by the exocyst subunits (Yue et al., 2017).

In a study conducted using polarized MDCK cells, the exocyst complex was found to selectively tether cargo vesicles that were directed toward the basolateral surface. Specifically, exocyst subunits Sec6, Sec8, and Exo70 localized to early endosomes, transferrin-positive common recycling endosomes, and Rab11a-positive apical recycling endosomes. When Sec8 was

blocked by antibodies, basolateral recycling, apical recycling, and basolateral-to-apical transcytosis were affected, suggesting exocyst requirements by several endocytic pathways. Namely, within transcytosis, the movement of apical recycling endosomes to the apical PM was sensitive to the function-blocking Sec8 antibodies. Although the inhibition was incomplete, suggesting a multiplicity of mechanisms affecting transcytosis, this also suggests a role that exocysts may have in mediating the transcytotic process (Oztan et al., 2007).

1.3.1.3 CD13 in Transcytosis

CD13 endocytosis has previously been studied in the context of viral entry. Specifically, CD13 acts as a receptor to bind human coronavirus 229E (HCoV-229E), and entry of HCoV-229E viral particles relied on sequestration of CD13 to a caveolin-1 positive region in human fibroblasts. Depletion of caveolin-1 reduced infection considerably, which suggests that caveolin-1 mediated endocytosis is necessary for entry of HCoV-229E bound to CD13 in this subset of cells (Bayati et al., 2021; Nomura et al., 2004). Alternatively, coronavirus transmissible gastroenteritis virus (TGEV), which relies on CD13 as receptors, was reported to undergo endocytosis in apical plasma membranes of MDCK cells using clathrin-coated pits (Delmas et al., 1992). The contrasting results of these experiments were appropriated to CD13 acting in different ways depending on the cell line, suggesting that CD13 relies on different forms of endocytosis depending on the species and cell line used (Nomura et al., 2004).

Upon entry of CD13, CD13 has been reported in the context of inflammatory responses as they have been observed to co-internalize with other proteins such as TLR4, CD14, and dynamin into $Rab5^{+}$ early endosomes. CD13 is necessary to negatively regulate TLR4 signaling in order to maintain inflammatory equilibrium and prevent accumulation of oxidative stress mediators and tissue injury by regulating the innate immune response (Ghosh et al., 2015). In addition, our lab

has already indicated that CD13 localization precedes and mediates apical protein trafficking by $Rab11^+$ and $Rab35^+$ recycling endosomes (Wang et al., 2021),

In terms of CD13 release, it has been suggested that in fibroblast like synoviocytes, release may be mediated in one of three ways: secretion through exocytosis, protease-mediated cleavage from the cell surface, and secretion on the surface of extracellular vesicles such as exosomes. Mechanisms surrounding the exocytosis of CD13 are not yet clear, suggesting that further studies need to be done (Morgan et al., 2016).

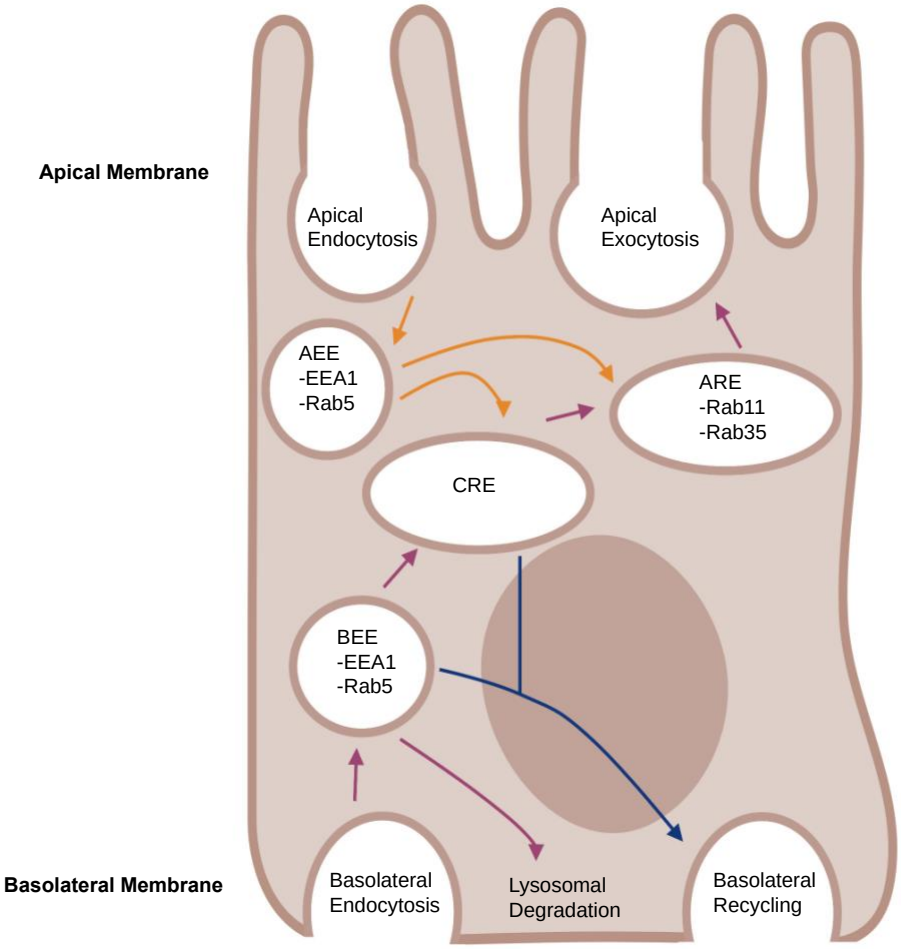

Figure 1.3.1 Illustrative representation of the transcytosis mechanism in epithelial cells. Proteins are internalized at the basolateral membrane or apical membrane through the endocytosis process. Basolateral proteins undergoing transcytosis are transported to Rab5- and EEA1-containing basolateral early endosomes (BEE) and are then sorted and delivered to lysosomes for degradation, to the basolateral surface for recycling, or to common recycling endosomes (CRE) for further progression of transcytosis. Proteins are then delivered to apical recycling endosomes (ARE), which are subsequently delivered to the apical membrane surface for exocytosis. Some apical proteins undergoing transcytosis are sorted to apical early endosomes (AEE), which are also

EEA1^{+} and Rab5^{+}. These proteins are cycled through the CRE to undergo basolateral exocytosis or directed to ARE for recycling at the apical surface. Illustration was modeled after (Fung et al., 2018) on Biorender.

1.4 Hypothesis and Project Aims

In previous findings by our lab, we determined that CD13 localization occurs prior to and independent of Rab11 and Rab35 enrichment, suggesting that it is not being localized through recycling endosomes, but rather earlier in the early endosomal process. In addition, transcytosis has been proposed to be responsible for transport of apical proteins (Mostov et al., 2000), and the first process of transcytosis involves markers of early endocytosis, notably early endosome antigen 1 (EEA1), which acts as a marker for the docking of incoming endocytic vesicles to early endosomes (Wilson et al., 2000). Given the localization of CD13 to the apical membrane, it became of interest to us to look at EEA1 in the context of CD13.

In addition, our lab determined that when CD13 was depleted, tyrosine 6 mutation in the cytoplasmic tail of CD13 was unable to restore correct apical polarity orientation. However, the mechanism of how this was occurring remained unknown (Wang et al., 2021). Recent studies looking into apical proteins like NgCAM suggest that its initial delivery and endocytosis to the basolateral membrane prior to being transcytosed depends on phosphorylation of tyrosine 33 on its cytoplasmic tail (Anderson et al., 2005).

In this project, I hypothesize that **early endosome antigen 1 (EEA1+)-positive vesicles and phosphorylation of tyrosine 6 on CD13 by src kinase are both necessary for the localization of CD13 to the cell-cell contact site prior to apical membrane specification**. These are the first steps that permit CD13 to initially insert at the basolateral membrane and undergo transcytosis

from the basolateral membrane towards the apical site. These steps are necessary to promote early polarization, which is fundamentally essential in lumen formation.

To test my hypothesis, I have 2 main aims:

AIM 1: Understand the role of EEA1+ mediated vesicles in CD13 delivery in early polarization steps

Immunofluorescence images of Caco-2 cells grown in 3D culture were analyzed to determine the effect of EEA1-depletion on CD13 localization.

AIM 2: Understand how phosphorylation of Tyrosine 6 impacts CD13 delivery in early polarization steps

Proximal ligation assays and immunofluorescence images of Caco-2 cells grown in 3D culture in the presence or absence of dasatinib, a src kinase inhibitor, were analyzed to determine the effect on CD13 localization.

2. Materials and Methods

2.1 DNA and shRNA Constructs

The pLX317-CD13-V5 plasmid was purchased from Sigma (TRCN, CD13 TRCN0000476147), and GFP-EEA1 wt plasmid was a gift from Silvia Corvera (Addgene plasmid #42307). pWPI-CD13-mCh was obtained by subcloning cDNA products to pWPI. pLX317-CD13^{Y6F}-V5 was generated using the QuikChange II site directed mutagenesis kit according to manufacturer's instructions (Agilent #200523).

shRNAs targeting human EEA1 and CD13 were cloned in pLKO. The following shRNAs were acquired from the McGill Platform for Cellular Perturbation (MPCP):

sh5CD13:CCGGGTGACCATAGAGTGGTGGAATCTCGAGATTCCACCACTCTATGGTCACTTTTTG,

sh4EEA1:CCGGCCCTTGAAAGTATCAAGCAAACTCGAGTTTGCTTGATACTTTCAAGGGTTTTT,

and a non-targeting scrambled shRNA was used as a control.

2.2 Cell Culture

The Caco-2 human intestinal epithelial cell line and HEK293LT human embryonic kidney cell line were purchased from American Type Culture Collection (ATCC). The cells were cultured at 37°C in 5% CO_2 in complete media, composed of DMEM (Wisent #319-005-CL) supplemented with 10% fetal bovine serum (Wisent 080-150), 100 U/ml penicillin, and 0.1mg/mL streptomycin (Wisent #450201EL). For 3D cyst culture, Caco-2 cells were seeded at a density of 1.0 x 10^4

cells/well in 8-well µ-slides (Ibidi 80826) coated with 100% GelTrex (ThermoFisher Scientific A1413202) in media supplemented with 2% GelTrex. Cells were collected for immunofluorescence after one or ten days in culture. For the dasatinib condition, Caco-2 cells were treated with 1uM dasatinib (ApexBio BMS-354825) 1 hour after being plated in 3D culture.

2.3 3D Cell Culture in Suspension

Low adhesion dishes were made by dissolving 2g of Poly-HEMA (Poly 2-hydroxyethyl methacrylate; Sigma Cat # P3932) in 100mL of 95% ethanol and rotating it for several hours at 65°C. 10 cm plates were then coated with 4mL of Poly-HEMA solution and dried overnight at 37°C. Caco-2 cells were first cultured at 37°C in 5% CO_2 in complete media, composed of DMEM (Wisent #319-005-CL) supplemented with 10% fetal bovine serum (Wisent 080-150), 100 U/ml penicillin, and 0.1mg/mL streptomycin (Wisent #450201EL). When Caco-2 cells were 80% confluent, media was aspirated, and cells were washed with 1x PBS twice and trypsinized for 5 min at 37°C using 0.25% Trypsin (Wisent, Cat# 325-043-EL). Cells were centrifuged and resuspended in 8mL of complete media supplemented with 2% Geltrex. The cells were then plated in the Poly-HEMA coated plates for 24-26 hours and collected.

2.4 Transient Transfection

HEK293LT cells were plated in 100mm dishes at 2.0 x 10^6 cells per dish and transfected with the appropriate plasmids using Polyethylenimine (PEI) as per manufacturer's instructions (Sigma #408727). Experiments using HEK293LT cells were performed 48 hours post-transfection. Caco-2 cells were plated in 6-well dishes at 2.0 x 10^5 cells per well and transfected with the appropriate plasmids using Lipofectamine LTX as per manufacturer's instructions (Invitrogen #15338030). Experiments using Caco-2 cells were performed 24 hours post-transfection.

2.5 Lentivirus Production

Lentivirus was produced by performing calcium phosphate transfection of HEK293LT cells in 6-well dishes with 3.3µg of lentiviral plasmid, 1µg of VSVG coat protein plasmid, pMD2.G, 2.5µg of packaging plasmid, psPAX2. Viral supernatants were collected after 48 hours and were aliquoted and frozen at -80°C. Caco-2 cells were infected with lentiviral supernatants and selected by adding 15ug/mL puromycin for 10 days.

2.6 Immunoprecipitation and Immunoblotting

Cells were washed twice with ice-cold PBS and lysed in NP40 buffer (150 mM NaCl, 1% NP-40, 50 mM Tris-HCl, pH 8.0) supplemented with 10mM NaF, 1mM NaVO4, calyculin A, and protease inhibitor cocktail. Lysates were precleared with MagnaBeads (Thermo Fisher Scientific #12321D) and then incubated with 2µg of antibody or IgG control overnight at 4°C. Antibodies were captured with MagnaBeads and washed three times with NP40 buffer. For immunoblotting, cells were lysed in RIPA lysis buffer (50 mM Tris-HCl, pH 8, 0.15 M NaCl, 0.1% SDS, 1% NP-40, 1% sodium deoxycholate, 50 mM NaF, 5 mM orthovanadate, 1 mM DTT) supplemented with proteinase inhibitor cocktail (Sigma # 11836170001). Total proteins were separated by SDS-PAGE, assessed with Ponceau Red, and transferred to Nitrocellulose membrane (Bio-rad # 1620115). The primary antibodies used were: α-Tubulin 1/5000 (Sigma #T9026), CD13 1/1000 (Abcam #ab108382), EEA1 1/1000 (BD Biosciences # 610457), mCherry 1/1000 (DSHB #3D5-s), Phospho-Tyrosine 1/1000 (Santa Cruz Biotechnology #sc-508), and mouse V5 1/5000 (ThermoFisher Scientific #R960-25). Data was analyzed using several programs including Excel and JMP16.

2.7 Immunostaining and Confocal Imaging

Caco-2 3D cysts were fixed with 2% paraformaldehyde/PBS for 10 min, permeabilized in 0.5% Triton X-100/10% Goat serum/10% fish gelatin/PBS for 1 hour, and subsequently incubated overnight in primary antibodies. For cysts treated with shrimp alkaline phosphatase (rSAP), cysts were treated with 10U/ul rSAP post-fixation, and permeabilized and blocked similar to other samples. The primary antibodies were used at the following dilutions: CD13 1/100 (Abcam #ab108382), E-cadherin 1/200 (Cell Signaling #3195S), EEA1 1/200 (BD Biosciences # 610457), Par6B (B-10) 1/100 (Santa Cruz Biotechnology #sc-166405), and Phalloidin 1/20 (Invitrogen #A34055). The secondary antibodies conjugated to Alexa488 (at 1:750), Alexa546 (at 1:750), or Alexa647 (at 1:200) (Jackson ImmunoResearch Laboratories). DNA was detected with Hoechst dye 33258. Confocal imaging was performed using the LSM700 from Zeiss with 20X/0.8NA or 40X/1.4NA objective lenses with a varying laser power range of 350-700nm, varying scan speeds of 7-9, and line averaging of 4. Images were then processed and analyzed using FIJI/ImageJ software.

2.8 Live Imaging

Live-imaging of Caco-2 3D structures was performed using a LSM700 confocal microscope with a LD plan-Neofluar 20X/0.4NA Korr M27 objective lens with ZEN software (Zeiss). Caco-2 cells were transiently transfected with CD13-mCherry and GFP-EEA1 in 2D cell culture. Cells were seeded in 3D culture prior to performing live imaging. For the dasatinib condition, Caco-2 cells were treated with 1uM dasatinib (ApexBio BMS-354825) 1 hour after being plated in 3D culture. Images were captured every 30 min with 7 slices (1μm) using two channels in an environmental chamber (37 °C, 5% CO2) for 3 days. Images were captured using solid state lasers (405, 488, 555, or 633nm), with scan speeds of 7-9, and line averaging of 4.

2.9 Proximity Ligation Assay

Caco-2 cells were first fixed in 2% (wt/vol) PFA for 20 minutes and permeabilized in 0.2% (vol/vol) Triton-X for 10 minutes. Blocking, hybridization with PLA probes, ligation and amplification were performed according to the manufacturer's protocol (DuoLink in situ, Sigma). Caco-2 cells were incubated using mouse anti-Phospho-Tyrosine antibody (Santa Cruz Biotechnology #sc-508) and rabbit anti-CD13 antibody (Abcam #ab108382). Confocal imaging was performed using the LSM700 from Zeiss with 40X/1.4NA objective lens, and images were processed and analyzed using FIJI/ImageJ software.

2.10 Statistical Analysis

For analysis of the overlap of CD13-Y6F puncta with EEA1 and CD13 with E-cadherin, local maxima were identified for using a cross-correlation function. To calculate cross-correlation, images were cropped to regions-of-interest containing areas of interest, and the background for each image was subtracted so that background pixels had a value of 0 using ImageJ. Pearson's Linear Correlation Coefficient (ρ) was calculated using MATLAB. The p-value was calculated by running 1000 simulations that randomized the position pixel/puncta positions for one channel. The proportion of simulations that had a higher correlation co-efficient than the sample was the p-value. Analysis of CD13 and E-Cadherin was also completed by identifying local maxima using a cross-correlation function. The area of interest, which was the cell-to-cell contact site, was defined by line tracing with a line thickness of 9 pixels, and the background for each image was subtracted so that background pixels had a value of 0 using ImageJ. Pearson's Linear Correlation Coefficient (ρ) was calculated using MATLAB. The p-value was calculated by running 1000 simulations that randomized the position pixel/puncta positions for one channel. Statistical analysis was conducted

by comparing two unpaired independent means using two-tailed t-tests, and p-values < 0.05 were considered significant. Data involving statistics were based on two replicates. The data was further analyzed using Excel and JMP16.

3. Results

3.1 CD13 associates with EEA1 during early apical membrane formation

Previous studies from our lab identified that CD13 was involved in early stages of apical membrane formation as it first established at the cell-cell contact site, followed by specification at the adhesion line, compacted accumulation at the AMIS, and furthermore, maturation into the PAP (Wang et al., 2021). To understand if $EEA1^+$ vesicles were implicated in mediating and localizing CD13 in these early steps, we examined endogenous CD13 and EEA1 expression at early timepoints of apical membrane formation, specifically in the 2-cell stage for Caco-2 cells cultured in 3D for 24 hours. We defined early apical membrane formation into different stages: early adhesion, late adhesion, and AMIS. Throughout these stages, we observed $EEA1^+$ vesicles aggregating predominantly towards the central region between the two cells and localizing to the sites of CD13 enrichment at each of the stages. The early adhesion stage was defined as EEA1+ vesicles being found both centrally and peripherally without the definition of CD13 at the adhesion line (Figure 1A, Upper Panel). Notably, at the early adhesion stage, E-cadherin was already defined at the adhesion line between the 2 cells (Figure 3.1.1A, Upper Panel). At the late adhesion stage, CD13 became enriched at the adhesion line between the 2 cells alongside E-cadherin, and we observed EEA1 expression aggregating and surrounding CD13 at this line (Figure 3.1.1A, Middle Panel). As CD13 condensed to form the AMIS, EEA1 was found to no longer be dispersed along the adhesion line, but rather, found concentrated around the AMIS site (Figure 3.1.1A, Lower Panel). To determine if EEA1 and CD13 could physically interact, CD13-V5 was overexpressed in HEK293 cells in order to immunoprecipitate V5 or IgG as control and immunoblot for EEA1. This identified that there was an approximately 7.5-fold greater enrichment relatively in the interaction between CD13 and EEA1 compared to control (Figure 3.1.1B). Our live imaging of

Caco-2 cells co-transfected with EEA1-GFP and CD13-mCherry further confirmed our findings of EEA1 and CD13 association during apical membrane formation as areas that were positive for CD13 were predominantly found to also be positive for EEA1+ vesicles. Specifically, the white arrow points to an example of an EEA1+ vesicle that is positive for CD13 moving and incorporating into the cyst structure during early polarization timepoints (Figure 3.1.1C). Therefore, these data demonstrate that CD13 can associate with EEA1 during early apical membrane formation.

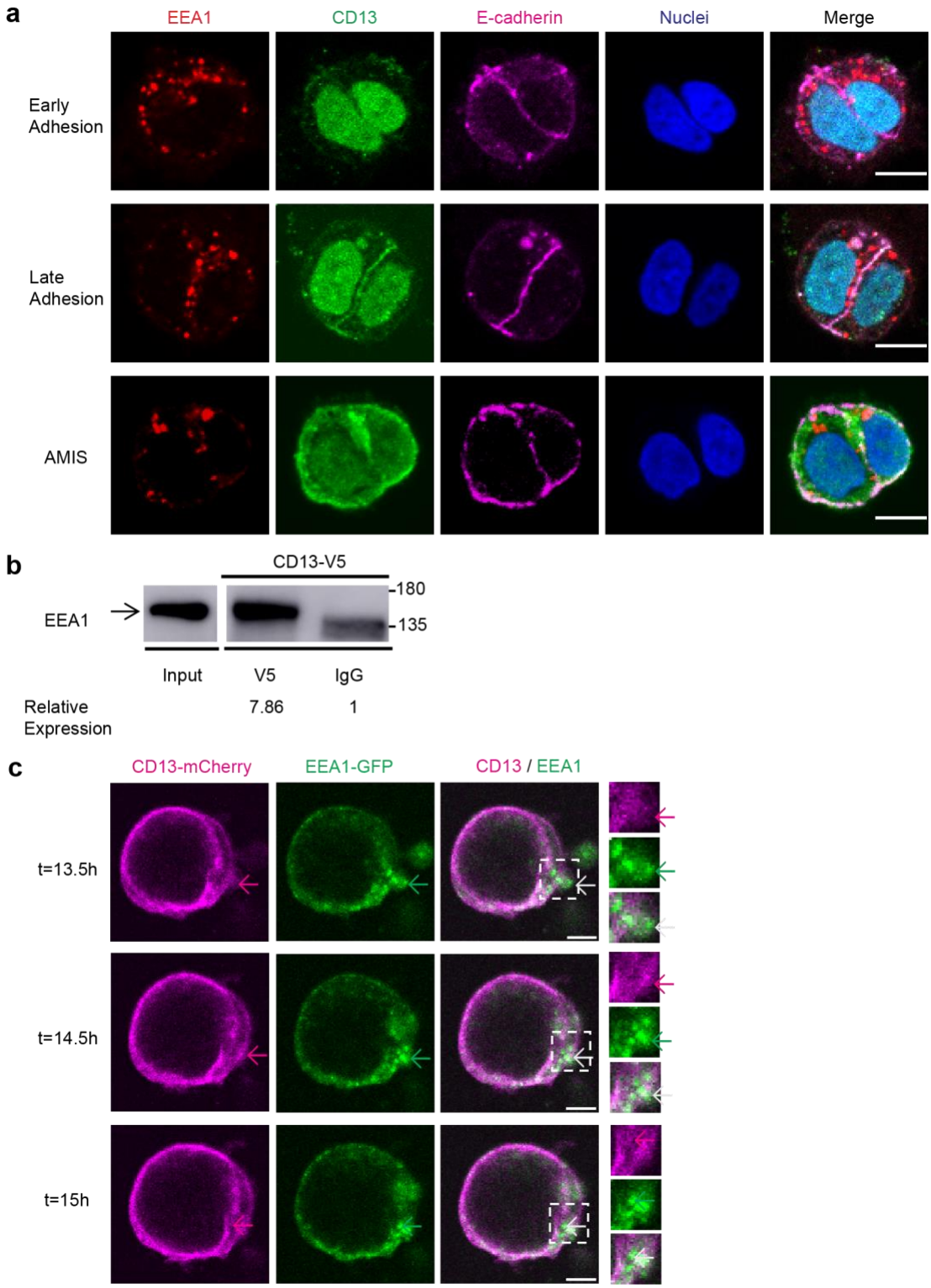
a
EEA1
CD13
E-cadherin
Nuclei
Merge
Early Adhesion
Late Adhesion
AMIS
b
CD13-V5
EEA1
180
135
Input
V5
IgG
Relative Expression
7.86
1
c
CD13-mCherry
EEA1-GFP
CD13 / EEA1
t=13.5h
t=14.5h
t=15h

Figure 3.1.1 EEA1 localizes near the apical domain of 3D Caco-2 during polarization. (A) Confocal images of Caco-2 cysts (10,000 cells/well) cultured for 24 hours immunostained for EEA1 (red), CD13 (green), and E-cadherin (magenta), showing the localization of EEA1, CD13, and E-cadherin at early adhesion, late adhesion, and AMIS stages. Note: the nuclear CD13 signal is non-specific staining, confirmed by validating anti-CD13 antibody in CD13 knockdown cells. Images are representative of 3 experimental replicates. (B) Immunoprecipitation was performed on HEK293 cell lysates transfected with CD13-V5 with IgG or anti-V5 and blotted for EEA1. Relative expression of two replicates was normalized to IgG and listed below. (C) Caco-2 cells (200,000 cells/well) were co-transfected to express CD13-mCherry and EEA1-EGFP in 2D culture and were subsequently plated in 3D culture (10,000 cells/well) to initiate cell polarization. Time-lapse confocal images were captured every 30 min, and these images were taken at 13.5h, 14.5h, and 15h respectively. Magenta, green, and white arrows demonstrate an example of an $EEA1^+$ and $CD13^+$ vesicle localizing within the cyst structure during early polarization timepoints. Live imaging results are representative of 2 experimental replicates. Scale bars: A, C, 10μm.

3.2 EEA1 is necessary for correct localization of CD13 in early apical membrane formation

To further explore the role of EEA1 in apical membrane initiation, we examined the consequences of EEA1-depletion by culturing control or shEEA1-4 Caco-2 cells for 24 hours in 3D culture. The efficiency of the shRNA promoting EEA1 knockdown was confirmed to decrease EEA1 expression by greater than 50% through Western blot (Figure 3.2.1A). Upon looking at the 2-cell stage, EEA1-depleted cells lacked central accumulation of CD13 at cell-cell contact sites whereas control cells (shScr) initiated early apical membrane formation and had progressed to its adhesion stage. E-cadherin remained constant in EEA1-depleted and control cysts (Figure 3.2.1B). Furthermore, to identify the impact of EEA1 in apical protein localization, EEA1-depleted cells

were stained for Par6 (Figure 3.2.1C). Our lab has previously reported that Par6 localizes centrally in the presence of CD13, whereas Par6 failed to accumulate centrally and was found on the outer edges in the context of CD13 depletion (Wang et al., 2021). Our results indicated that in control cysts, Par6 accumulated at the cell-cell contact site as expected, whereas with EEA1-depletion, Par6 was displaced throughout the cell or found peripherally and failed to accumulate centrally (Figure 3.2.1C). EEA1-depleted cells were then cultured for a 10-day duration in 3D culture in addition to CD13-depleted cells for phenotypic reference and shScr cells as control (Figure 3.2.1D). Phenotypically, EEA1-depleted cysts mimicked CD13-depleted cysts in forming solid structures, whereas the control cysts formed prominent lumen (Figure 3.2.1D). There was a significant reduction in lumen formation in EEA1-depleted cysts (Figure 3.2.1E), further suggesting that EEA1 is necessary in the early steps to orient CD13 properly.

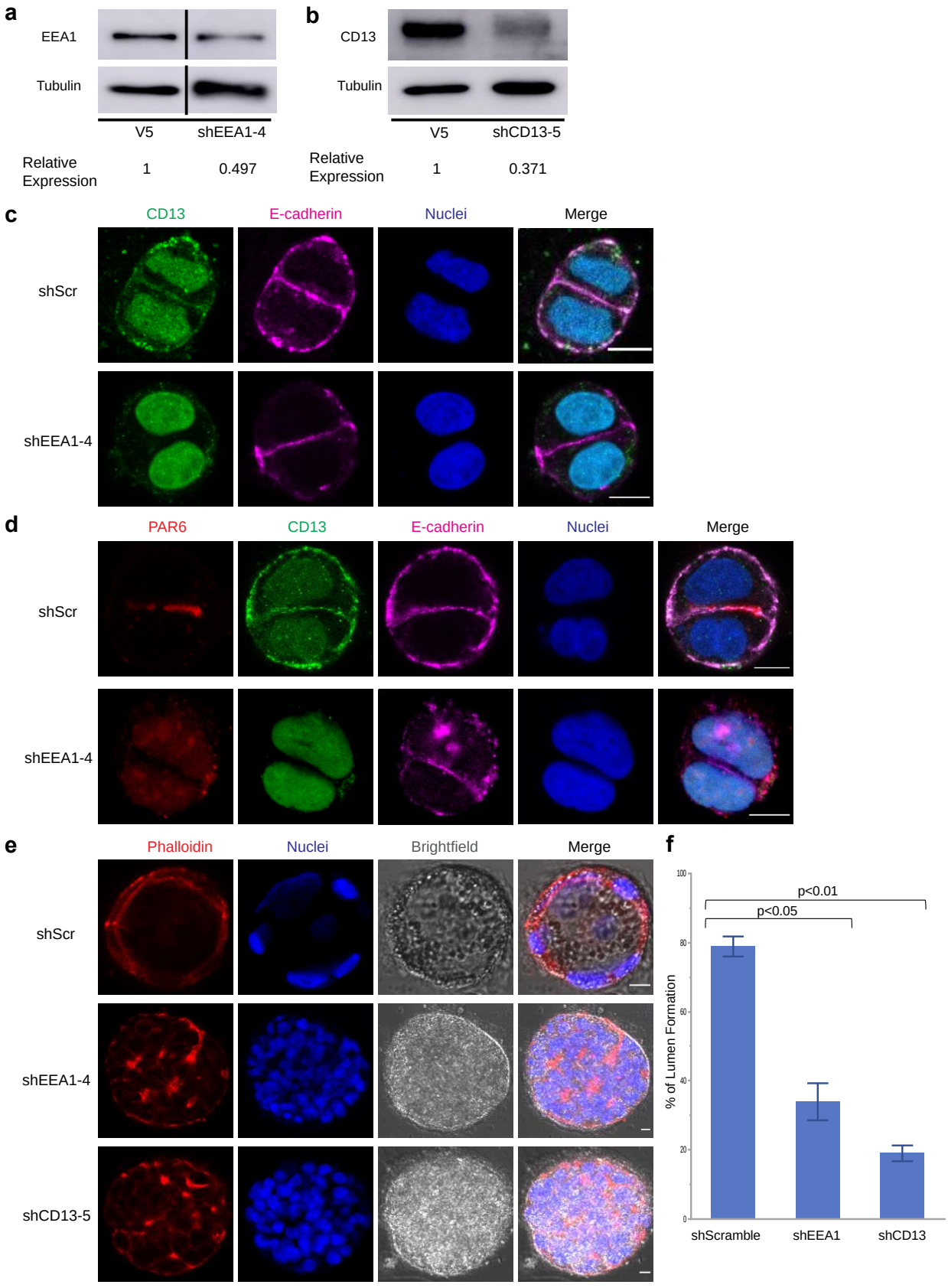
a
EEA1
Tubulin
V5
shEEA1-4
Relative Expression
1
0.497
b
CD13
Tubulin
V5
shCD13-5
Relative Expression
1
0.371
c
CD13
E-cadherin
Nuclei
Merge
shScr
shEEA1-4
d
PAR6
CD13
E-cadherin
Nuclei
Merge
shScr
shEEA1-4
e
Phalloidin
Nuclei
Brightfield
Merge
shScr
shEEA1-4
shCD13-5
f
p<0.01
p<0.05
% of Lumen Formation
100
80
60
40
20
0
shScramble
shEEA1
shCD13

Figure 3.2.1 EEA1 knockdown disrupts CD13 function to orient apical-basal polarity. (A) Left- Caco-2 cells were transfected with shEEA1-4 or shScr (control) prior to collection of cell lysates. Western blotting was performed on cell lysates with anti-EEA1 antibody to visualize knockdown efficiency. (B) Caco-2 cells were transfected with shCD13-5 or shScr (control) prior to collection of cell lysates. Western blotting was performed on cell lysates with anti-CD13 antibody to visualize knockdown efficiency. (C) Confocal images of Caco-2 cysts expressing shScr or shEEA1-4 cultured for 24 hours and immunostained for CD13 (green) and E-cadherin (magenta) at adhesion stage. (D) Confocal images of Caco-2 cysts treated with shScr or shEEA1-4 cultured for 24 hours and immunostained for Par6 (red), CD13 (green), and E-cadherin (magenta) at the late adhesion stage. (E) Confocal images of Caco-2 cysts treated with shScr, shEEA1-4, or shCD13-5 cultured for 10 days and immunostained for Phalloidin (red). (F) Quantification of cysts with single prominent lumen in shScr (n=79), shEEA1-4 (n=77), and shCD13-5 (n=52) treated Caco-2 cysts cultured in 3D for 10 days. Results are from 2 independent experiments, and error bars represent standard errors. Scale bars: B-D, 10μm.

3.3 CD13-Y6F colocalizes with EEA1^{+} vesicles

Tyrosine (Y6) within the intracellular domain was previously reported as necessary for several non-catalytic functions of CD13 (Subramani et al., 2013). Previous studies conducted in our lab have suggested that this residue is necessary to establish orientation of apical-basal polarity in Caco-2 cysts in CD13-depleted cells. Cells with other point mutations within the CD13 intracellular domain were able to restore polarity orientation, suggesting the specificity of the tyrosine residue. In addition, our lab observed that CD13-Y6F was localized and trapped in intracellular puncta. Upon examining a marker for the endoplasmic reticulum (calreticulin), it was found that only about 20% of CD13 puncta colocalized with this site (Wang et al., 2021). From

this, we then became interested to see if CD13-Y6F puncta were being trapped in $EEA1^+$ vesicles, so we immunostained to examine colocalization of CD13-Y6F and EEA1. In CD13-Y6F-expressing cells with endogenous wild-type CD13, EEA1 localized in a similar manner to WT Caco-2 cells as vesicles gathered towards the cell-cell contact site, aggregated towards CD13 upon specification at the adhesion line, and condensed as CD13 condensed at the AMIS, indicating that correct apical polarity orientation was maintained (Figure 3.3.1A). However, in CD13-depleted CD13-Y6F cells, EEA1 failed to accumulate centrally, and CD13 seemed to be trapped in these $EEA1^+$ vesicles, which were unable to be delivered to the site of cell-cell contact (Figure 3.3.1A). Upon analysis of the correlation between EEA1 and CD13, it was determined that while EEA1 colocalized with about 10% of CD13 puncta in control cells, CD13-Y6F cysts showed that $EEA1^+$ vesicles colocalized with about 90% of CD13 into intracellular puncta (Figure 3.3.1B). This identified that the majority of CD13-Y6F was likely being trapped in $EEA1^+$ vesicles, rather than being able to localize correctly to the site of cell-cell contact to begin adhesion and AMIS development.

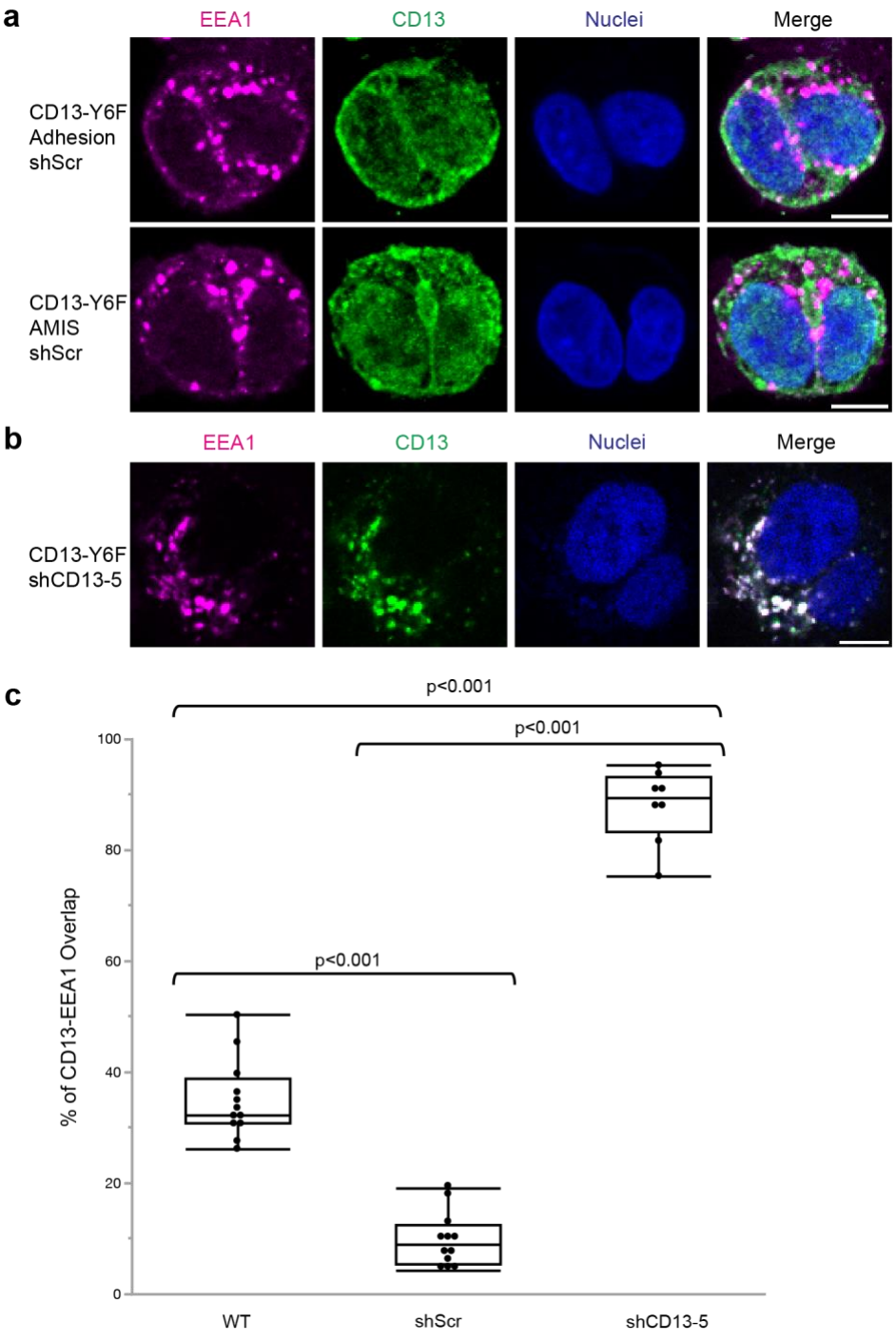
a
EEA1
CD13
Nuclei
Merge
CD13-Y6F
Adhesion
shScr
CD13-Y6F
AMIS
shScr
b
EEA1
CD13
Nuclei
Merge
CD13-Y6F
shCD13-5
c
p<0.001
p<0.001
p<0.001
% of CD13-EEA1 Overlap
100
80
60
40
20
0
WT
shScr
shCD13-5

Figure 3.3.1 Mutation of tyrosine 6 to phenylalanine in the intracellular domain of CD13 promotes trapping in EEA1$^+$ vesicles. (A) Confocal images of CD13-Y6F mutant Caco-2 cysts treated with shScr cultured for 24 hours and immunostained for EEA1 (red) and CD13 (green) at adhesion and AMIS stages. (B) Confocal images of CD13-Y6F mutant Caco2 cysts treated with shCD13-5 cultured for 24 hours and immunostained for EEA1 (red) and CD13 (green). (C) Quantification of the proportion of CD13 puncta that overlap with positive puncta of EEA1 in CD13-Y6F mutant Caco2 cysts treated with shScr or shCD13-5. Dots represent the percentage of correlation between EEA1 and CD13 in individual Caco-2 structures. Scale bars: A, B, 10μm.

3.4 CD13 becomes tyrosine phosphorylated in vesicles prior to mobilizing to adhesions

With the understanding that the mutation of tyrosine 6 within the intracellular domain of CD13 prevents correct mobilization of CD13, we then conducted proximity ligation assays to assess if phosphorylation of tyrosine is implicated in the mobilization and further accumulation of CD13 at the site of cell-cell contact for progression into early apical membrane formation. We assayed cysts using antibodies against Phospho-tyrosine (P-Tyr) and CD13 to identify interactions among these two targets. After Caco-2 cysts were grown for 24 hours, we discovered interactions of P-Tyr and CD13 centrally and peripherally at the 2-cell stage, which was reminiscent of the pre-adhesion stage (Figure 3.4.1A, Upper Panel). After cysts were grown for 30 hours, puncta of interaction between these two targets were seen to accumulate predominantly at the site of cell-cell contact, which was reminiscent of the adhesion stage (Figure 3.4.1A, Lower Panel). The puncta of interaction were reminiscent of vesicles that were being mobilized with each subsequent stage. Then, we treated these Caco-2 cysts with dasatinib, an inhibitor for site-specific tyrosine phosphorylation by Src kinases, 1 hour after plating cells in 3D culture. We observed that interactions of P-Tyr and CD13 were diminished as noted by the number of puncta, and the puncta

were located peripherally rather than at cell-cell contact site (Figure 3.4.1B). As a control, we treated Caco-2 cysts with shrimp alkaline phosphatase (rSAP), known to remove 5'-phosphates from DNA, RNA, and proteins, after fixation to confirm that tyrosine phosphorylation was required for a positive result in this assay. Indeed, we observed a diminished number of puncta and lack of puncta found at the site of cell-cell contact (Figure 3.4.1C). Upon quantification of puncta in the 2-cell stage of Caco-2 cysts, we determined that the mean number of puncta found in WT cysts was 11 whereas cysts treated with dasatinib or rSAP had a mean of 3 puncta (Figure 3.4.1D). Then, we performed analysis on the number of puncta that were found between the two nuclei (at cell-cell contact site) compared to the number of puncta found peripherally around the two nuclei. In WT cysts, there was a slightly greater number of puncta found centrally than peripherally, whereas with dasatinib and rSAP controls, this difference was much more drastic, with the minimal number of puncta being found on the peripheral sides of the nuclei (Figure 3.4.1E). Finally, to further identify interaction of P-Tyr with CD13, CD13-V5 was overexpressed in Caco-2 cells, and cell lysates were then collected in order to immunoprecipitate P-Tyr or IgG as control and immunoblot for V5. This identified that there was an approximately 3-fold greater enrichment in the interaction between P-Tyr and CD13 compared to control (Figure 3.4.1F).

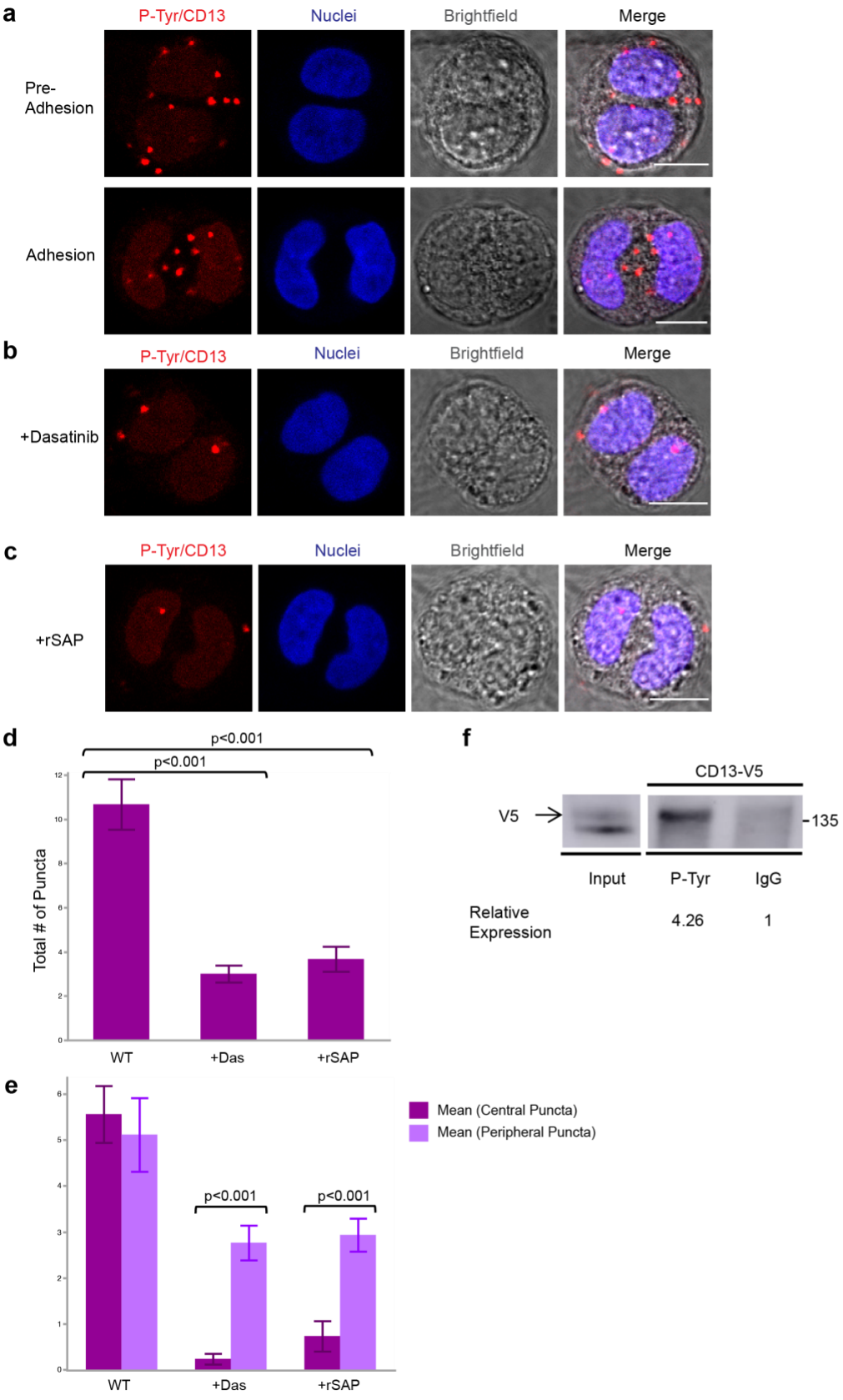
a
P-Tyr/CD13
Nuclei
Brightfield
Merge
Pre-Adhesion
Adhesion
b
+Dasatinib
c
+rSAP
d
p<0.001
p<0.001
Total # of Puncta
WT
+Das
+rSAP
e
Mean (Central Puncta)
Mean (Peripheral Puncta)
p<0.001
p<0.001
f
CD13-V5
V5
135
Input
P-Tyr
IgG
Relative Expression
4.26
1

Figure 3.4.1 Tyrosine phosphorylation of CD13 occurs in vesicles prior to early apical membrane formation. (A) Confocal images of Caco-2 cells cultured in 3D following proximity ligation assay using anti-P-Tyr and anti-CD13 antibodies. Interactions of P-Tyr and CD13 were visualized and quantified as discrete red puncta. The upper panel demonstrates cyst after being cultured in 3D for 24 hours where cyst is found in the pre-adhesion stage, in which puncta are localized centrally and peripherally. The lower panel demonstrates cysts after being cultured in 3D for 30 hours where cysts were at the adhesion stage, in which puncta are concentrated at cell-cell contact site. (B) Confocal images of Caco-2 cells cultured in 3D for 30 hours and treated with dasatinib (1uM) undergone proximity ligation assay using anti-P-Tyr and anti-CD13 antibodies. Interactions of P-Tyr and CD13 are visualized and quantified as discrete red puncta. (C) Confocal images of Caco-2 cells cultured in 3D for 30 hours and treated with rSAP post-fixation (10U/ul) undergone proximity ligation assay using anti-P-Tyr and anti-CD13 antibodies. Interactions of P-Tyr and CD13 were visualized and quantified as discrete red puncta. (D) Quantifications of total puncta of individual Caco-2 cysts in WT (n=18), dasatinib (n=20), and rSAP (n=14) conditions as seen in confocal images. (E) Quantifications of central and peripheral puncta of individual Caco-2 cysts respectively in WT (n=18), dasatinib (n=20), and rSAP (n=14) conditions as seen in confocal images. (F) Immunoprecipitation was performed on Caco2 cells transfected with CD13-V5 and cultured in 3D suspension method with IgG or anti-P-Tyr and blotted for V5. Ponceau staining of tubulin was used as loading control. The graph below shows the quantification of band intensities. Scale bars: A-C, 10μm.

3.5 Dasatinib treatment results in loss of central CD13 and EEA1 accumulation, preventing early apical membrane formation

To further understand the role of src kinases in phosphorylating tyrosine 6 in the intracellular domain of CD13, Caco-2 cysts were treated with dasatinib 1 hour after plating cells into 3D culture. Cysts were then fixed and immunostained 24 hours after, and control cysts were those that were not treated with dasatinib. In cysts with dasatinib treatment, CD13 was no longer found at the cell-cell contact site (Figure 3.5.1, Lower Panel). EEA1, which was found to concentrate and surround CD13 along the adhesion line in control cysts (Figure 3.5.1A, Upper Panel) also failed to accumulate at the cell-cell contact site of treated cells (Figure 3.5.1A, Lower Panel). EEA1 was found to be dispersed along the periphery of nuclei (Figure 3.5.1A, Lower Panel). The expression of E-cadherin along the adhesion line remained consistent in both treatment and control cysts (Figure 3.5.1A). Results from live-imaging of Caco-2 cells transfected with EEA1-GFP and CD13-mCherry suggested that dasatinib was impacting early apical membrane formation. In contrast to the non-dasatinib condition in which a large association between EEA1 and CD13 was observed (Figure 3.1.1C), EEA1+ vesicles were shown to be distributed diffusely within the dasatinib-treated cyst, and largely, these EEA1+ vesicles did not seem to associate with CD13, further indicating the impact of phosphorylation in early polarization steps (Figure 3.5.1B).

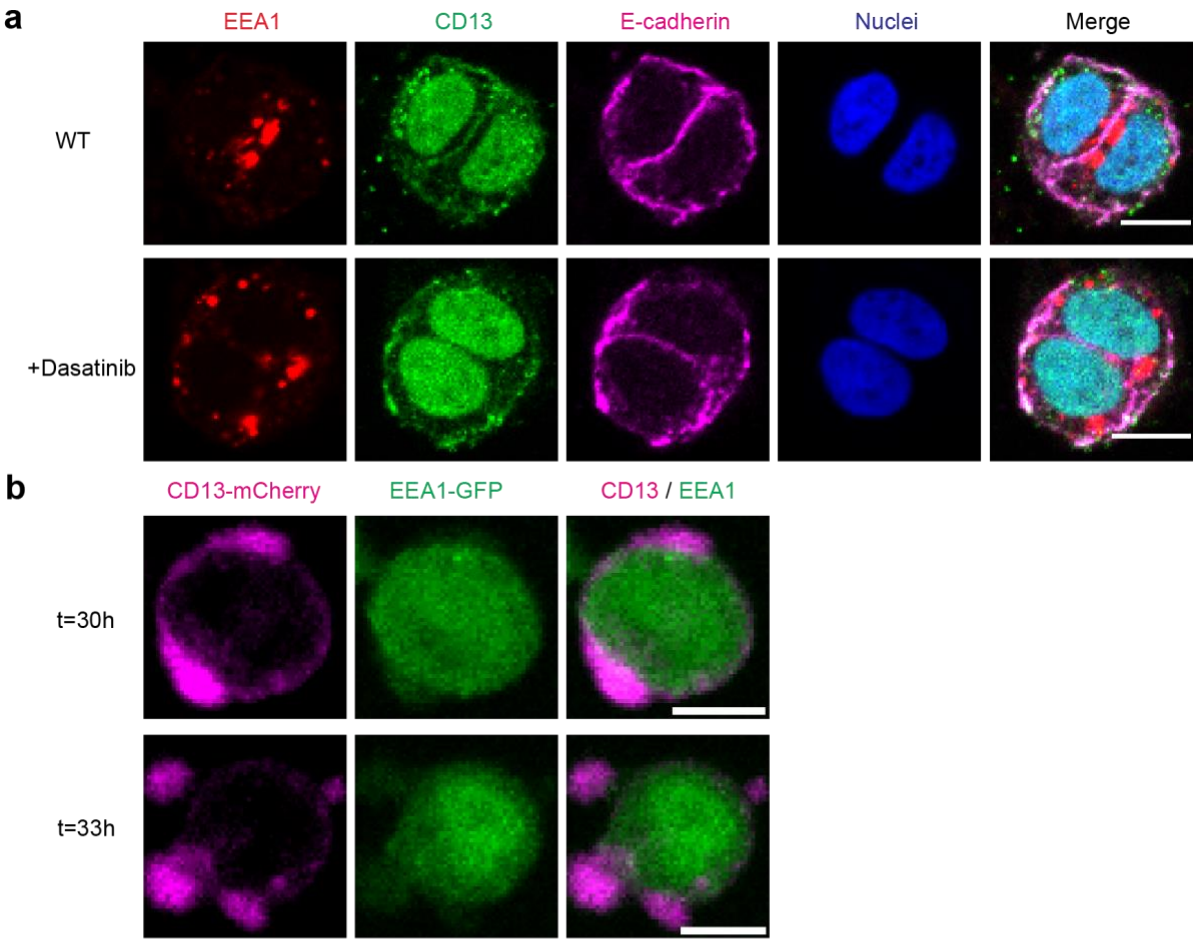
a
EEA1
CD13
E-cadherin
Nuclei
Merge
WT
+Dasatinib
b
CD13-mCherry
EEA1-GFP
CD13 / EEA1
t=30h
t=33h

Figure 3.5.1 Dasatinib prevents CD13 accumulation required for apical membrane formation. (A) Confocal images of WT Caco-2 cells cultured in 3D for 24 hours with or without treatment of dasatinib (1uM) and immunostained for EEA1 (red), CD13 (green), and E-cadherin (magenta) at the adhesion stage. (B) Caco-2 cells were transfected to express CD13-mCherry and EEA1-EGFP in 2D culture and were subsequently plated in 3D culture to initiate cell polarization. Cells were treated with dasatinib (1uM) 1h after plating in 3D. Time-lapse confocal images were captured every 30 min, and these images were taken at 30h and 33h respectively. Scale bars: A-B 10μm.

3.6 CD13 progression through the stage of early apical membrane formation simultaneously promotes pushing and lateral spreading of E-cadherin

Our lab has previously investigated the roles of various polarity proteins in the context of epithelial cells, including CD13 and E-cadherin. CD13 localizes to the apical membrane while E-cadherin localizes to the basolateral membrane (Wang et al., 2021). However, what remains elusive is how CD13 and E-cadherin localization become mutually exclusive after colocalizing at the adhesion. In the adhesion stage, we observed CD13 and E-cadherin co-existing at the adhesion line (Figure 3.6.1A). Upon further analysis, we observed a high correlation of CD13 and E-cadherin at the adhesion stage, with a correlation coefficient of 0.7499 (Figure 3.6.1B, G). As cells progressed to the AMIS stage, which was characterized by accumulation of CD13, E-cadherin expression was diminished at the AMIS (Figure 3.6.1C). The correlation coefficient at the AMIS was 0.0977, which was remarkably low (Figure 3.6.1D, G). Notably, E-cadherin expression was the highest at the points adjacent to the CD13 accumulation at the AMIS, and expression decreased as it moved further away from the AMIS (Figure 3.6.1D). The correlation coefficient at the cell-cell contact site was -0.339, demonstrating that CD13 and E-cadherin become negatively

correlated with further development of the apical membrane (Figure 3.6.1G). Moving towards the pre-apical patch (PAP) stage, which was characterized by the maturation of the AMIS, we observed CD13 expression further accumulating and elongating while E-cadherin became further diminished and restricted towards the periphery of the cell (Figure 3.6.1E). Upon analysis of the correlation coefficient, CD13 and E-cadherin were further negatively correlated with a value of -0.7408 (Figure 3.6.1F, G).

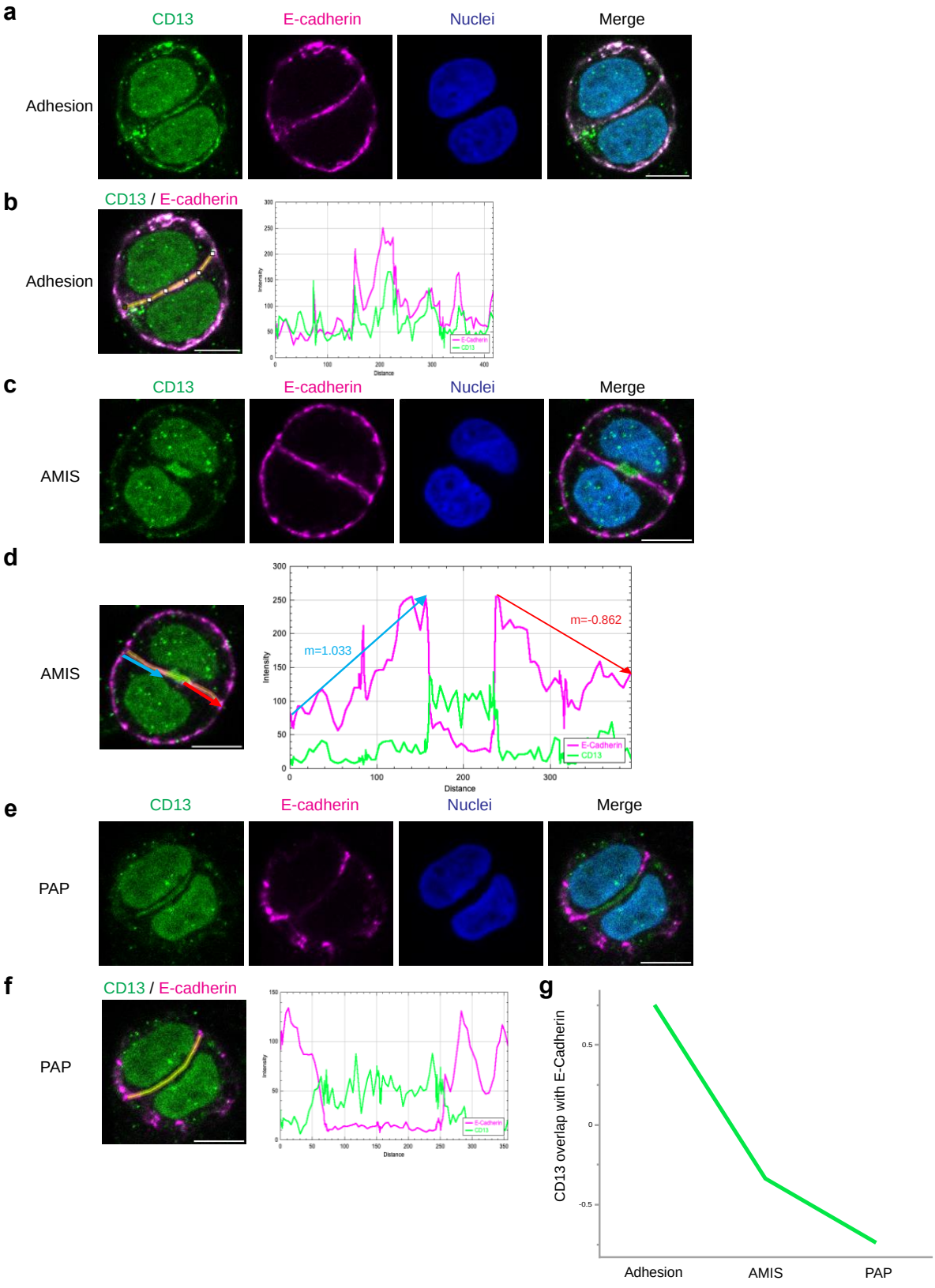
a
CD13
E-cadherin
Nuclei
Merge
Adhesion
b
CD13 / E-cadherin
Adhesion
Intensity
Distance
E-Cadherin
CD13
c
CD13
E-cadherin
Nuclei
Merge
AMIS
d
AMIS
m=1.033
m=-0.862
Intensity
Distance
E-Cadherin
CD13
e
CD13
E-cadherin
Nuclei
Merge
PAP
f
CD13 / E-cadherin
PAP
Intensity
Distance
E-Cadherin
CD13
g
CD13 overlap with E-Cadherin
Adhesion
AMIS
PAP

Figure 3.6.1 Functions of CD13 and E-cadherin during early apical specification of Caco-2 cells. (A) Confocal images of Caco-2 cysts cultured in 3D for 24 hours and immunostained for CD13 (green) and E-cadherin (magenta) at adhesion stage. (B) Left: Specification of the line at adhesion used to determine intensities of CD13 and E-cadherin at the given location. Right: Graph of intensities of CD13 and E-cadherin along the distance of the cell-cell contact site. (C) Confocal images of Caco-2 cysts cultured in 3D for 24 hours and immunostained for CD13 (green) and E-cadherin (magenta) at the AMIS stage. (D) Left: Specification of line at cell-cell contact site used to determine intensities of CD13 and E-cadherin at AMIS stage. The blue arrow specifies E-cadherin expression from one end of the periphery to the AMIS. The red arrow specifies E-cadherin expression from the AMIS to the other end of the periphery. Right: Graph of intensities of CD13 and E-cadherin along the cell-cell contact site. The blue arrow indicates the slope of E-cadherin expression from one end of the periphery to the AMIS. The red arrow indicates the slope of E-cadherin expression from AMIS to the other end of the periphery. (E) Confocal images of Caco-2 cysts cultured in 3D for 24 hours and immunostained for CD13 (green) and E-cadherin (magenta) at the PAP stage. (F) Left: Specification of line used to determine intensities of CD13 and E-cadherin along PAP. Right: Graph of intensities of CD13 and E-cadherin along the distance of PAP. (G) Graph of correlation coefficients between CD13 and E-cadherin at the stages of adhesion, AMIS, and PAP. Scale bars: A-F, 10μm.

4. Discussion, Future Directions, Conclusion

4.1 Discussion

In this study, our results demonstrate that EEA1 mediates CD13 during epithelial lumen formation by directing CD13 in the early apical-basal polarity orientation steps. Silencing EEA1 in Caco-2 cysts is characterized by a lack of CD13 accumulation at the cell-cell contact site, preventing initiation of apical specification by CD13. Furthermore, EEA1 depletion results in a similar inverted polarity phenotype as found in CD13 depleted cysts, characterized as apical complexes being positioned at the periphery of cell aggregates rather than basolateral proteins. We also identify the requirement of tyrosine phosphorylation at the intracellular domain of CD13 within vesicles in order for CD13 to localize correctly to initiate apical specification. Upon inhibition of tyrosine phosphorylation, as seen in cysts treated with dasatinib, CD13 is unable to mobilize to the site of cell-cell contact, phenotypically mimicking cysts with EEA1 depletion. Finally, we identify a relationship between CD13 and E-cadherin in early polarization steps as it progresses from co-existing at adhesion to CD13 accumulating centrally while simultaneously pushing E-cadherin to the outer periphery of the cell. Here, we provide further understanding on the early cellular functions involving CD13 localization, which are critical for CD13 to assert its function in orienting apical-basal polarity for proper tissue function and epithelial homeostasis.

EEA1 has been reported to be present in complex endosomal pathways in both polarized and nonpolarized cells by docking incoming endocytic vesicles before fusion with early endosomes (Wilson et al., 2000). In the context of polarity, EEA1 has been implicated in targeting and delivery of several proteins through a transcytotic manner in EEA1+ vesicles from the basolateral membrane to the apical membrane (Anderson et al., 2005; Bidaud-Meynard et al., 2019). Past studies in our lab focused on the role of CD13 in late endosome recycling but given that CD13

accumulation at the future apical membrane site preceded Rab11 and Rab35, which are key proteins mediating apical endosome recycling, we sought to see if CD13 localization was occurring through an early endosomal process in early polarization steps (Wang et al., 2021). My results indicate that EEA1 mediates CD13 through various stages of early apical membrane formation noted by accumulation of EEA1 in CD13-enriched areas. $EEA1^+$ vesicles surrounded CD13 as it became enriched along the adhesion line at the adhesion stage, and after progression to the AMIS stage, $EEA1^+$ vesicles displaced towards CD13 accumulation and were no longer found evenly distributed along the adhesion line, suggesting a role of $EEA1^+$ vesicles in mediating CD13 localization. Furthermore, our imaging data revealed that EEA1 depletion in the 2-cell stage resulted in an absence of CD13 localization during apical membrane initiation, suggesting that $EEA1^+$ vesicles are needed for correct delivery of CD13. There is currently no known interaction of EEA1 and E-cadherin, a well-established marker of the basolateral membrane, and this is further suggested in my data as the displacement of E-cadherin remains undisrupted along the cell-cell contact site (Nelson et al., 2013). It then became of interest to us to observe Par6 localization in the context of EEA1 depletion given that our lab previously observed Par6 being retained at the cell periphery and being excluded from the cytoplasm in CD13-depleted cells (Wang et al., 2021). Our results indicated that Par6 was unable to accumulate, indicating that disruption of $EEA1^+$ vesicles at polarity initiation prevented trafficking of apical proteins at later stages. Finally, the results in this thesis demonstrate that EEA1 depleted cells had diminished ability for lumen formation. Solid cysts that were formed as a result of depletion phenocopied CD13-depleted cysts, indicating $EEA1^+$ vesicle delivery of CD13 is necessary and acts as a preceding step in apical membrane establishment.

The involvement of $EEA1^+$ vesicles in apical protein transport has been extensively reported, specifically in epithelial transcytosis of integral membrane proteins, which are first trafficked to the basolateral membrane and destined for the apical surface (Mostov & Simister, 1985; Schaerer et al., 1991). A useful model to study basolateral-to-apical transcytosis has been the trafficking mechanism of polymeric immunoglobulin receptor (pIgR). As part of the mucosal immune response, pIgR binds to dimeric IgA (dIgA) prior to internalization through clathrin-mediated endocytosis in MDCK epithelial cells (Mostov et al., 1992). This is followed by recruitment and activation of Src family kinase, p62Yes, which further leads to phosphorylation and activation of downstream proteins involved in pIgR transcytosis (Luton et al., 1999). The IgA-receptor complex is delivered to basolateral early endosomal compartments, noted by the colocalization of EEA1 and Rab5 at these endosomes (Bucci et al., 1994; Leung et al., 2000). The cargo is then processed by common recycling endosomes to be directed to the lysosomes for degradation, recycled back to the basolateral surface, or mediated towards the apical region for exocytosis (Brown et al., 2000; E. Wang et al., 2000). The mechanism behind the route that dIgA-pIgR takes for exocytosis is yet unclear. One hypothesis suggests that they are directed for exocytosis directly by common recycling endosomes at the apical membrane. The other suggests that complexes are sorted to Rab11-, Rab17-, and Rab25- containing apical recycling endosomes prior to delivery to the apical membrane for exocytosis (James E. Casanova et al., 1999; X. Wang et al., 2000; Zacchi et al., 1998). Proteins like cystic fibrosis transmembrane conductance receptor (CFTR) relies on $EEA1^+$ endosomes as well but follow a slightly different mechanism to the trafficking of pIgR. Unlike pIgR that are processed by common recycling endosomes, the commitment of CFTR to the apical membrane precedes entry of cargo into $Rab5^+$ and $EEA1^+$ basolateral early endosomes (Bidaud-Meynard et al., 2019). In addition, the transcytosis of CFTR was independent of N-glycans, AP-

1B, Rab3b, Rab17, Rab25, and the exocyst complex, which are essential for apical transcytosis of proteins like pIgR (Hunziker & Peters, 1998; Nelms et al., 2017; Perez Bay et al., 2013; van Ijzendoorn et al., 2002). Finally, transcytosis of CFTR mostly avoided the use of common recycling endosomes and apical recycling endosomes, which are frequently implicated in transcytosis of other cargo (Jerdeva et al., 2010; Lalioti et al., 2016). Given our lab's previous work has implicated the role of CD13 in mediating apical protein trafficking through apical recycling endosomes, it raises the possibility that the mechanism behind CD13 localization through transcytosis closely follows the trafficking mechanism of pIgR (Wang et al., 2021).

In our previous study, our lab reported that in the absence of wildtype CD13, mutation of Tyr 6 in the intracellular domain of CD13 (CD13-Y6F) results in CD13 being locked in a vesicular compartment, which further prevents its ability to translocate to the plasma membrane, a necessary process for correct polarity orientation. In CD13, tyrosine 6 is phosphorylated in a Src- dependent manner (Subramani et al., 2013). Given that the staining pattern of CD13-Y6F was reminiscent of ER, CD13, observed to be localized to intracellular puncta, was previously assessed to see if its retention was occurring as a result of the ER. The results indicated that while there was a moderate effect on ER retention, the majority of CD13 was not being accounted for (Wang et al., 2021). My work adds to this, demonstrating that the majority of CD13-Y6F resides in $EEA1^{+}$ vesicles. Together, these results indicate that phosphorylation of Y6 is necessary for efficient trafficking of CD13.

Overall, src-family kinases seem to be implicated in trafficking of apical proteins at the entry point when proteins are initially delivered to a membrane for endocytosis. For pIgR, binding to dIgA led to recruitment and activation of P62Yes, a Src family kinase in epithelial cells, and this led to the downstream activation of proteins to promote endocytosis of the complex at the

basolateral membrane and promotion of the transcytotic process (Luton et al., 1999; Mostov et al., 1992). For NgCAM, initial delivery and endocytosis at the basolateral membrane within epithelial cells relied on tyrosine 33 in the cytoplasmic tail. It was proposed that NgCAM relied on phosphorylation of tyrosine 33 by a src-family kinase to undergo basolateral targeting (Anderson et al., 2005). Src-family kinases have been implicated in the internalization process for endothelial transcytosis as well. Transcytosis studies of albumin, which has critical functions in maintaining transendothelial oncotic pressure gradients and transporting bloodborne substances such as lipids, hormones, and peptides, have proposed that endothelial internalization of albumin relied on Src-family kinases to mediate phosphorylation of caveolin-1 and GTPase dynamin2 (Schnitzer et al., 1988; Schnitzer et al., 1994; Shajahan et al., 2004). Src-induced phosphorylated and activated dynamin to bind to caveolin-1, promoting recruitment of caveolae, which were determined necessary for albumin endocytosis (Shajahan et al., 2004). In addition, low density lipoproteins (LDL), implicated in cardiovascular health, have been determined to undergo transcytosis in endothelial cells (Dehouck et al., 1997). LDL is internalized through caveolae-mediated, clathrin-mediated, or caveolin and clathrin-independent endocytosis at the apical membrane (Fung et al., 2018). LDL is then subjected to degradation in lysosomes or is mediated by activin receptor-like kinase 1 (ALK1) receptors and scavenger receptor B1 (SR-B1) for transcytosis to the basolateral membrane (Zhu et al., 2008). Similar to albumin transcytosis, endothelial transcytosis of LDL relies on caveolae-mediated entry, and although the mechanism remains uncertain, it is speculated that src kinases are implicated at the caveolae-level through effects on caveolin-1 in the endocytosis process (Fung et al., 2018).

Given the implication of tyrosine and src-family kinases during early endosomal timepoints at endocytosis, our current study aimed to look at the co-localization of EEA1 and CD13 to assess if

$EEA1^+$ vesicles were the vesicular compartments locking in CD13. Our results suggest that the majority of CD13-Y6F puncta are trapped in EEA1+ vesicles and that the tyrosine in the intracellular domain is playing a role in localizing CD13 correctly, presumably at the initial basolateral domain to undergo transcytosis.

Tyrosine residues of the cytoplasmic tail have been found to be critical in targeting apical proteins to the initial basolateral domain for transcytosis. Absence of phosphorylation by src kinases on these tyrosine residues has been shown to prevent transcytosis and inhibit displacement of these proteins to the apical membrane (Anderson et al., 2005). Based on our results with CD13-Y6F being trapped in intracellular puncta, we hypothesized that CD13 was acting in a similar manner, requiring phosphorylation on the Tyr 6 for correct delivery to the cell-cell contact site to begin early polarization steps. Our proximity ligation assay results support our hypothesis as we observed puncta of interaction between anti-CD13 and anti-P-Tyr antibodies in WT Caco-2 cysts, indicative of CD13 phosphorylation. In several cysts, the puncta were localized dispersedly around the cell, which were reminiscent of the early adhesion stage in which CD13 had not accumulated yet to the cell-cell contact site. In cysts that had undergone further progression of apical membrane formation, the puncta were localized centrally between the nuclei, which were reminiscent of $EEA1^+$ vesicles surrounding the CD13-enriched adhesion line during the late adhesion stage. Cysts, treated with dasatinib, a src-family kinase inhibitor, displayed decreased puncta of interaction between CD13 and P-Tyr, and these puncta were subjected to the outer periphery of the nuclei, suggesting that phosphorylation is necessary for localizing CD13 to the cell-cell contact site for apical membrane specification. Puncta found in cysts treated with phosphatase phenocopied cysts treated with dasatinib, further verifying that P-Tyr is necessary for CD13 localization in early polarization steps. Further specificity verification of this PLA assay can be

done by repeating this experiment using Caco-2 cells treated with CD13 shRNA. The residual puncta in the periphery following dasatinib or rSAP treatment could reflect that some sites may be inaccessible for dephosphorylation; however, it seems likelier that these treatments are effective in depleting interaction rather than inhibiting interaction completely. A study looking at P-Tyr expression to assess its posttranslational modifying effect on cancer, specifically in K562 leukemia cells, used PLAs to follow the dynamics of P-Tyr protein localization. Here, they treated cells with imatinib, a tyrosine kinase inhibitor, to identify any measurable differences of P-Tyr. Imatinib decreased the P-Tyr levels significantly compared to the P-Tyr expression in the WT PLA, but it was unable to abolish all activity, which was similar to our PLA results (Elfineh et al., 2014). It is also important to note that although PLA allows quantification of interaction as discrete spots, the strength of interaction cannot be assessed because fluorescence of each of these spots cannot be compared to one another. Therefore, despite our data suggesting some signal in dasatinib and rSAP conditions, resulting in residual puncta, Tyr may be weakly phosphorylated, resulting in weak interaction between P-Tyr and CD13. This could be why these puncta are subjected to the periphery and unable to access the cell-cell contact site, which is necessary for apical membrane specification.

It is important to address that there are other limitations to using PLAs due to the assay showing proximity rather than direct events occurring on CD13. Given the vast functions of CD13 to act in roles such as receptors, enzymes, and signaling molecules, and the various ligands that CD13 has been shown to associate with, such as matrix metalloproteinases and carbohydrate moieties such as galectin-4, we cannot completely exclude the possibility that CD13 is binding to another protein that is tyrosine phosphorylated (Ghaffari et al., 2010; Mina-Osorio, 2008; Mina-Osorio et al., 2007). In addition, although detection of interaction between P-Tyr and CD13 can

be quantified, proximity ligation assays do not reveal site specific information as to where this interaction is occurring. However, our imaging data of Caco-2 cysts treated with dasatinib further support our findings from the proximity ligation assays and promote the notion that CD13 is the protein undergoing phosphorylation. Inhibition of phosphorylation resulted in an absence of CD13 localization during apical membrane initiation, suggesting that phosphorylation is necessary for delivery of CD13 to the cell-cell contact site. Furthermore, cysts treated with dasatinib phenotypically mimicked cysts with EEA1 depletion, marked by absence of CD13 between the two nuclei.

Previous studies involving apical protein localization through transcytosis, specifically the necessity of src-family kinase-dependent phosphorylation for internalization of apical proteins into EEA1-mediated early endosomes, and our current results involving mislocalization of CD13 in conditions of EEA1 depletion, CD13-Y6F mutation, and src-family kinase inhibition all suggest a specific, novel mechanism by which CD13 is localizing in early polarization steps. CD13 exists in vesicles that are $EEA1^{+}$, and prior to delivery to the cell-cell contact site, CD13 undergoes phosphorylation within these vesicles, notably at Tyrosine 6 of the intracellular domain. CD13 relies on vesicles being $EEA1^{+}$ and phosphorylation to be able to localize correctly to begin apical membrane formation. In the absence of either one, CD13 is unable to contribute to its function of orienting apical-basal polarity.

In the 2-cell stage of Caco-2 cysts, CD13, a protein that localizes apically, colocalized with E-cadherin, which is a well-established marker of the basolateral membrane (Nelson et al., 2013). Our imaging data demonstrates an initial correlative relationship between CD13 and E-cadherin at the adhesion stage but demonstrates a subsequent change as the relationship becomes anti-correlative as CD13 and E-cadherin progress through the AMIS and PAP stages. Interestingly, as

E-cadherin displaces peripherally simultaneously to CD13 accumulation in AMIS and PAP stages, we observe that the fluorescent expression of E-cadherin is brightest at sites closest to CD13. This seems indicative of CD13 'pushing' E-cadherin outwardly as it accumulates centrally; however, the mechanism directing this remains unknown.

4.2 Future Directions

Our results identify a novel mechanism detailing how $EEA1^+$ vesicles and phosphorylation of the CD13 intracellular domain allow for it to correctly localize for initiation of apical membrane establishment. EEA1, as mentioned, acts as a marker to dock incoming endocytic vesicles prior to fusion with early endosomes (Wilson et al., 2000). EEA1 has been reported to be involved in proper delivery of transcytotic endosomes to the apical membrane (Bidaud-Meynard et al., 2019; Wilson et al., 2000), which has effectively been a basis of this study. However, it must be noted that transcytosis requires endocytic pathways but also possesses exocyst requirements to selectively tether cargo vesicles directed towards the target surface. Specifically, movement of early endosomes, apical recycling endosomes, and transferrin-positive common recycling endosomes all required components of the exocyst complex such as Sec6, Sec8, and Exo70 to ensure proper delivery to the apical membrane (Oztan et al., 2007). Therefore, future studies in this project should assess the function of the exocyst and identify whether depletion of exocyst complexes prevent correct localization of CD13.

Other future directions in this project should look at how this novel mechanism involving EEA1 and CD13 phosphorylation are implicated in the context of disease. Specifically, our lab has identified that polarity can be re-established in transformed cells. Re-introduction of CD13 to cancerous cells expressing various oncogenes promotes proper polarity in these cells and prevents them from maintaining a malignant phenotype, characterized by epithelial structures lacking

prominent lumen. Given the fact that cysts expressing EEA1 depletion phenocopies cancerous cells by disrupting lumen formation, it would be impactful to see how EEA1 and phosphorylation of the intracellular domain of CD13 are implicated within cancerous cells. In addition, our preliminary data indicate that re-introduction of CD13 reverts malignant phenotype, and therefore, it would be of interest for this project to see if EEA1 and phosphorylation of CD13 are then able to restore function as a result.

Finally, our results suggest an anti-correlative relationship between CD13 and E-cadherin as cysts progress through its early polarization steps. We highlight that E-cadherin is specifically enriched in areas that are neighboring CD13 during AMIS and PAP stages and hypothesize that as CD13 accumulates, it pushes E-cadherin out of the emerging apical zone, thus restricting it to the periphery. By assessing live-imaging of CD13 and E-cadherin, we would better be able to understand the dynamics that are involved to have a more comprehensive understanding of early apical-basal polarity.

4.3 Conclusion

The data presented in this thesis provide a crucial missing piece into understanding the early mechanism by which CD13 localizes to begin apical membrane establishment. Based on these results, I conclude that the intracellular domain of CD13 requires phosphorylation within $EEA1^{+}$ vesicles to target and deliver CD13 correctly. My work sets the foundation to further uncover how CD13 may be mediated through a transcytotic mechanism. In addition, my work opens up various avenues for projects that focus on looking at this novel mechanism in the context of disease such as cancer, potentially revealing novel targets to help establish potential therapeutics.

5. Bibliography

Ahmed, S. M., & Macara, I. G. (2017). The Par3 polarity protein is an exocyst receptor essential for mammary cell survival. *Nature communications*, *8*(1), 1-15.

Ahmed, S. M., Nishida-Fukuda, H., Li, Y., McDonald, W. H., Gradinaru, C. C., & Macara, I. G. (2018). Exocyst dynamics during vesicle tethering and fusion. *Nature communications*, *9*(1), 1-17.

Albiston, A. L., McDowall, S. G., Matsacos, D., Sim, P., Clune, E., Mustafa, T., . . . Connolly, L. M. (2001). Evidence that the angiotensin IV (AT4) receptor is the enzyme insulin-regulated aminopeptidase. *Journal of Biological Chemistry*, *276*(52), 48623-48626.

Altschul, S. F., Madden, T. L., Schäffer, A. A., Zhang, J., Zhang, Z., Miller, W., & Lipman, D. J. (1997). Gapped BLAST and PSI-BLAST: a new generation of protein database search programs. *Nucleic acids research*, *25*(17), 3389-3402. https://doi.org/10.1093/nar/25.17.3389

Anderson, E., Maday, S., Sfakianos, J., Hull, M., Winckler, B., Sheff, D., . . . Mellman, I. (2005). Transcytosis of NgCAM in epithelial cells reflects differential signal recognition on the endocytic and secretory pathways. *The Journal of cell biology*, *170*(4), 595-605. https://doi.org/10.1083/jcb.200506051

Archibald, A., Al-Masri, M., Liew-Spilger, A., & McCaffrey, L. (2015). Atypical protein kinase C induces cell transformation by disrupting Hippo/Yap signaling. *Molecular biology of the cell*, *26*(20), 3578-3595.

Aroeti, B., Kosen, P. A., Kuntz, I. D., Cohen, F. E., & Mostov, K. E. (1993). Mutational and secondary structural analysis of the basolateral sorting signal of the polymeric immunoglobulin receptor. *The Journal of cell biology*, *123*(5), 1149-1160. https://doi.org/10.1083/jcb.123.5.1149

Ballard, S. T., Trout, L., Mehta, A., & Inglis, S. K. (2002). Liquid secretion inhibitors reduce mucociliary transport in glandular airways. *American Journal of Physiology-Lung Cellular and Molecular Physiology*, *283*(2), L329-L335.

Bauvois, B. (2004). Transmembrane proteases in cell growth and invasion: new contributors to angiogenesis? *Oncogene*, *23*(2), 317-329. https://doi.org/10.1038/sj.onc.1207124

Bayati, A., Kumar, R., Francis, V., & McPherson, P. S. (2021). SARS-CoV-2 infects cells after viral entry via clathrin-mediated endocytosis. *Journal of Biological Chemistry*, *296*.

Bhartur, S. G., Calhoun, B. C., Woodrum, J., Kurkjian, J., Iyer, S., Lai, F., & Goldenring, J. R. (2000). Genomic Structure of Murine Rab11 Family Members. *Biochemical and Biophysical Research Communications*, *269*(2), 611-617. https://doi.org/https://doi.org/10.1006/bbrc.2000.2334

Bidaud-Meynard, A., Bossard, F., Schnúr, A., Fukuda, R., Veit, G., Xu, H., & Lukacs, G. L. (2019). Transcytosis maintains CFTR apical polarity in the face of constitutive and mutation-induced basolateral missorting. *Journal of cell science*, *132*(10), jcs226886. https://doi.org/10.1242/jcs.226886

Bilder, D. (2003). PDZ domain polarity complexes. *Current Biology*, *13*(17), R661-R662. https://doi.org/https://doi.org/10.1016/S0960-9822(03)00599-2

Bilder, D., Li, M., & Perrimon, N. (2000). Cooperative Regulation of Cell Polarity and Growth by Drosophila Tumor Suppressors. *Science*, *289*(5476), 113-116. https://doi.org/10.1126/science.289.5476.113

Bilder, D., Schober, M., & Perrimon, N. (2003). Integrated activity of PDZ protein complexes regulates epithelial polarity. *Nature Cell Biology*, *5*(1), 53-58. https://doi.org/10.1038/ncb897

Bostwick, D. G., & Cheng, L. (2012). Precursors of prostate cancer. *Histopathology*, *60*(1), 4-27.

Brown, P. S., Wang, E., Aroeti, B., Chapin, S. J., Mostov, K. E., & Dunn, K. W. (2000). Definition of distinct compartments in polarized Madin–Darby canine kidney (MDCK) cells for membrane-volume sorting, polarized sorting and apical recycling. *Traffic*, *1*(2), 124-140.

Bryant, D. M., Datta, A., Rodriguez-Fraticelli, A. E., Peränen, J., Martin-Belmonte, F., & Mostov, K. E. (2010). A molecular network for de novo generation of the apical surface and lumen. *Nature cell biology*, *12*(11), 1035-1045.

Bucci, C., Wandinger-Ness, A., Lütcke, A., Chiariello, M., Bruni, C. B., & Zerial, M. (1994). Rab5a is a common component of the apical and basolateral endocytic machinery in polarized epithelial cells. *Proceedings of the National Academy of Sciences*, *91*(11), 5061-5065.

Buono, N. L., Parrotta, R., Morone, S., Bovino, P., Nacci, G., Ortolan, E., . . . Funaro, A. (2011). The CD157-integrin partnership controls transendothelial migration and adhesion of human monocytes. *Journal of Biological Chemistry*, *286*(21), 18681-18691.

Butler, M. T., & Wallingford, J. B. (2017). Planar cell polarity in development and disease. *Nat Rev Mol Cell Biol*, *18*(6), 375-388. https://doi.org/10.1038/nrm.2017.11

Casanova James, E., Breitfeld Philip, P., Ross Stuart, A., & Mostov Keith, E. (1990). Phosphorylation of the Polymeric Immunoglobulin Receptor Required for Its Efficient Transcytosis. *Science*, *248*(4956), 742-745. https://doi.org/10.1126/science.2110383

Casanova, J. E., Apodaca, G., & Mostov, K. E. (1991). An autonomous signal for basolateral sorting in the cytoplasmic domain of the polymeric immunoglobulin receptor. *Cell*, *66*(1), 65-75. https://doi.org/https://doi.org/10.1016/0092-8674(91)90139-P

Casanova, J. E., Wang, X., Kumar, R., Bhartur, S. G., Navarre, J., Woodrum, J. E., . . . Goldenring, J. R. (1999). Association of Rab25 and Rab11a with the apical recycling system of polarized Madin-Darby canine kidney cells. *Molecular biology of the cell*, *10*(1), 47-61. https://doi.org/10.1091/mbc.10.1.47

Casanova, J. E., Wang, X., Kumar, R., Bhartur, S. G., Navarre, J., Woodrum, J. E., . . . Goldenring, J. R. (1999). Association of Rab25 and Rab11a with the apical recycling system of polarized Madin–Darby canine kidney cells. *Molecular biology of the cell*, *10*(1), 47-61.

Castellano, E., & Downward, J. (2011). RAS interaction with PI3K: more than just another effector pathway. *Genes & cancer*, *2*(3), 261-274.

Catterall, R., Lelarge, V., & McCaffrey, L. (2020). Genetic alterations of epithelial polarity genes are associated with loss of polarity in invasive breast cancer [https://doi.org/10.1002/ijc.32691]. *International Journal of Cancer*, *146*(6), 1578-1591. https://doi.org/https://doi.org/10.1002/ijc.32691

Chalmers, A. D., Pambos, M., Mason, J., Lang, S., Wylie, C., & Papalopulu, N. (2005). aPKC, Crumbs3 and Lgl2 control apicobasal polarity in early vertebrate development. *Development*, *132*(5), 977-986. https://doi.org/10.1242/dev.01645

Chatterjee, S. J., Halaoui, R., & McCaffrey, L. (2016). Apical–Basal Polarity as a Sensor for Epithelial Homeostasis: A Matter of Life and Death. *Current Pathobiology Reports*, *4*(3), 99-106. https://doi.org/10.1007/s40139-016-0107-5

Chatterjee, S. J., & McCaffrey, L. (2014). Emerging role of cell polarity proteins in breast cancer progression and metastasis. *Breast Cancer (Dove Med Press)*, *6*, 15-27. https://doi.org/10.2147/BCTT.S43764

Chen, C.-L., Gajewski, K. M., Hamaratoglu, F., Bossuyt, W., Sansores-Garcia, L., Tao, C., & Halder, G. (2010). The apical-basal cell polarity determinant Crumbs regulates Hippo signaling in Drosophila. *Proceedings of the National Academy of Sciences*, *107*(36), 15810-15815.

Chen, J., & Zhang, M. (2013). The Par3/Par6/aPKC complex and epithelial cell polarity. *Experimental Cell Research*, *319*(10), 1357-1364. https://doi.org/https://doi.org/10.1016/j.yexcr.2013.03.021

Chen, J.-K., Zimpelmann, J., Harris, R. C., & Burns, K. D. (2001). Angiotensin IV induces tyrosine phosphorylation of focal adhesion kinase and paxillin in proximal tubule cells. *American Journal of Physiology-Renal Physiology*, *280*(6), F980-F988.

Choi, J., Park, J.-H., Kwon, O. Y., Kim, S., Chung, J. H., Lim, D. S., . . . Han, Y. S. (2005). T-type calcium channel trigger p21ras signaling pathway to ERK in Cav3. 1-expressed HEK293 cells. *Brain research*, *1054*(1), 22-29.

Christoforidis, S., McBride, H. M., Burgoyne, R. D., & Zerial, M. (1999). The Rab5 effector EEA1 is a core component of endosome docking. *Nature*, *397*(6720), 621-625. https://doi.org/10.1038/17618

Chuderland, D., & Seger, R. (2005). Protein-protein interactions in the regulation of the extracellular signal-regulated kinase. *Molecular biotechnology*, *29*(1), 57-74.

Danziger, R. S. (2008). Aminopeptidase N in arterial hypertension. *Heart Failure Reviews*, *13*(3), 293-298. https://doi.org/10.1007/s10741-007-9061-y

Dehouck, B., Fenart, L., Dehouck, M.-P., Pierce, A., Torpier, G., & Cecchelli, R. (1997). A new function for the LDL receptor: transcytosis of LDL across the blood–brain barrier. *The Journal of cell biology*, *138*(4), 877-889.

Delgrossi, M.-H., Breuza, L., Mirre, C., Chavrier, P., & Le Bivic, A. (1997). Human syntaxin 3 is localized apically in human intestinal cells. *Journal of cell science*, *110*(18), 2207-2214.

Delmas, B., Gelfi, J., L'Haridon, R., Vogel, L. K., Sjöström, H., Norén, O., & Laude, H. (1992). Aminopeptidase N is a major receptor for the entero-pathogenic coronavirus TGEV. *Nature*, *357*(6377), 417-420. https://doi.org/10.1038/357417a0

Delmas, B., Gelfi, J., Sjöström, H., Noren, O., & Laude, H. (1994). Further characterization of aminopeptidase-N as a receptor for coronaviruses. In *Coronaviruses* (pp. 293-298). Springer.

Dossus, L., & Benusiglio, P. R. (2015). Lobular breast cancer: incidence and genetic and non-genetic risk factors. *Breast cancer research : BCR*, *17*, 37-37. https://doi.org/10.1186/s13058-015-0546-7

Drivas, G. T., Shih, A., Coutavas, E. E., D'Eustachio, P., & Rush, M. G. (1991). Identification and characterization of a human homolog of the Schizosaccharomyces pombe ras-like gene YPT-3. *Oncogene*, *6*(1), 3-9.

Drubin, D. G., & Nelson, W. J. (1996). Origins of cell polarity. *Cell*, *84*(3), 335-344.

Dunn, K. W., McGraw, T. E., & Maxfield, F. R. (1989). Iterative fractionation of recycling receptors from lysosomally destined ligands in an early sorting endosome. *The Journal of cell biology*, *109*(6), 3303-3314.

Elfineh, L., Classon, C., Asplund, A., Pettersson, U., Kamali-Moghaddam, M., & Lind, S. B. (2014). Tyrosine phosphorylation profiling via in situ proximity ligation assay. *BMC cancer*, *14*(1), 1-8.

Elsum, I., Yates, L., Humbert, P. O., & Richardson, H. E. (2012). The Scribble–Dlg–Lgl polarity module in development and cancer: from flies to man. *Essays in Biochemistry*, *53*, 141-168. https://doi.org/10.1042/bse0530141

Elsum, I. A., & Humbert, P. O. (2013). Localization, not important in all tumor-suppressing properties: a lesson learnt from scribble. *Cells Tissues Organs*, *198*(1), 1-11.

Farmen, S. L., Karp, P. H., Ng, P., Palmer, D. J., Koehler, D. R., Hu, J., . . . Welsh, M. J. (2005). Gene transfer of CFTR to airway epithelia: low levels of expression are sufficient to correct Cl− transport and overexpression can generate basolateral CFTR. *American Journal of Physiology-Lung Cellular and Molecular Physiology*, *289*(6), L1123-L1130.

Ferrari, A., Veligodskiy, A., Berge, U., Lucas, M. S., & Kroschewski, R. (2008). ROCK-mediated contractility, tight junctions and channels contribute to the conversion of a preapical patch into apical surface during isochoric lumen initiation. *Journal of cell science*, *121*(21), 3649-3663.

Frémont, S., & Echard, A. (2018). Membrane Traffic in the Late Steps of Cytokinesis. *Current Biology*, *28*(8), R458-R470. https://doi.org/https://doi.org/10.1016/j.cub.2018.01.019

Fung, K. Y. Y., Fairn, G. D., & Lee, W. L. (2018). Transcellular vesicular transport in epithelial and endothelial cells: Challenges and opportunities. *Traffic*, *19*(1), 5-18.

Ghaffari, A., Li, Y., Kilani, R. T., & Ghahary, A. (2010). 14-3-3σ associates with cell surface aminopeptidase N in the regulation of matrix metalloproteinase-1. *Journal of Cell Science*, *123*(17), 2996-3005.

Ghosh, M., Subramani, J., Rahman, M. M., & Shapiro, L. H. (2015). CD13 restricts TLR4 endocytic signal transduction in inflammation. *The Journal of immunology*, *194*(9), 4466-4476.

Ghosh, R. N., Gelman, D. L., & Maxfield, F. R. (1994). Quantification of low density lipoprotein and transferrin endocytic sorting HEp2 cells using confocal microscopy. *Journal of cell science*, *107*(8), 2177-2189.

Ghosh, R. N., & Maxfield, F. R. (1995). Evidence for nonvectorial, retrograde transferrin trafficking in the early endosomes of HEp2 cells. *The Journal of Cell Biology*, *128*(4), 549-561.

Goldenring, J. R., Smith, J., Vaughan, H. D., Cameron, P., Hawkins, W., & Navarre, J. (1996). Rab11 is an apically located small GTP-binding protein in epithelial tissues. *American Journal of Physiology-Gastrointestinal and Liver Physiology*, *270*(3), G515-G525. https://doi.org/10.1152/ajpgi.1996.270.3.G515

Gonzalez, L., & Scheller, R. H. (1999). Regulation of membrane trafficking: structural insights from a Rab/effector complex. *Cell*, *96*(6), 755-758.

Gonzalez-Mariscal, L., Betanzos, A., Nava, P., & Jaramillo, B. E. (2003). Tight junction proteins. *Progress in biophysics and molecular biology*, *81*(1), 1-44.

Halaoui, R., & McCaffrey, L. (2015). Rewiring cell polarity signaling in cancer. *Oncogene*, *34*(8), 939-950. https://doi.org/10.1038/onc.2014.59

Hamilton, T. A., Handa, R. K., Harding, J. W., & Wright, J. W. (2001). A role for the angiotensin IV/AT4 system in mediating natriuresis in the rat. *Peptides*, *22*(6), 935-944.

Handa, R. K. (2001). Characterization and signaling of the AT4 receptor in human proximal tubule epithelial (HK-2) cells. *Journal of the American Society of Nephrology*, *12*(3), 440-449.

Hegen, M., Kameoka, J., Dong, R. P., Schlossman, S. F., & Morimoto, C. (1997). Cross-linking of CD26 by antibody induces tyrosine phosphorylation and activation of mitogen-activated protein kinase. *Immunology*, *90*(2), 257-264.

Hirose, T., Izumi, Y., Nagashima, Y., Tamai-Nagai, Y., Kurihara, H., Sakai, T., . . . Ohno, S. (2002). Involvement of ASIP/PAR-3 in the promotion of epithelial tight junction formation. *Journal of Cell Science*, *115*(12), 2485-2495. https://doi.org/10.1242/jcs.115.12.2485

Hirt, R. P., Hughes, G. J., Frutiger, S., Michetti, P., Perregaux, C., Poulain-Godefroy, O., . . . Kraehenbuhl, J.-P. (1993). Transcytosis of the polymeric Ig receptor requires phosphorylation of serine 664 in the absence but not the presence of dimeric IgA. *Cell*, *74*(2), 245-255. https://doi.org/https://doi.org/10.1016/0092-8674(93)90416-N

Hooper, N. M. (1994). Families of zinc metalloproteases. *FEBS letters*, *354*(1), 1-6.

Huang, L., & Muthuswamy, S. K. (2010). Polarity protein alterations in carcinoma: a focus on emerging roles for polarity regulators. *Current opinion in genetics & development*, *20*(1), 41-50. https://doi.org/10.1016/j.gde.2009.12.001

Hunziker, W., & Peters, P. J. (1998). Rab17 localizes to recycling endosomes and regulates receptor-mediated transcytosis in epithelial cells. *Journal of Biological Chemistry*, *273*(25), 15734-15741.

Hémar, A., Olivo, J.-C., Williamson, E., Saffrich, R., & Dotti, C. G. (1997). Dendroaxonal transcytosis of transferrin in cultured hippocampal and sympathetic neurons. *Journal of Neuroscience*, *17*(23), 9026-9034.

Ikonen, E., & Simons, K. (1998). Protein and lipid sorting from thetrans–Golgi network to the plasma membrane in polarized cells.

Ivanov, A. I., Nusrat, A., & Parkos, C. A. (2004). Endocytosis of epithelial apical junctional proteins by a clathrin-mediated pathway into a unique storage compartment. *Molecular biology of the cell*, *15*(1), 176-188. https://doi.org/10.1091/mbc.e03-05-0319

Jahn, R., & Scheller, R. H. (2006). SNAREs—engines for membrane fusion. *Nature reviews Molecular cell biology*, *7*(9), 631-643.

Jedd, G., Mulholland, J., & Segev, N. (1997). Two new Ypt GTPases are required for exit from the yeast trans-Golgi compartment. *The Journal of cell biology*, *137*(3), 563-580.

Jerdeva, G. V., Tesar, D. B., Huey-Tubman, K. E., Ladinsky, M. S., Fraser, S. E., & Bjorkman, P. J. (2010). Comparison of FcRn-and pIgR-mediated transport in MDCK cells by fluorescence confocal microscopy. *Traffic*, *11*(9), 1205-1220.

Jewett, C. E., & Prekeris, R. (2018). Insane in the apical membrane: Trafficking events mediating apicobasal epithelial polarity during tube morphogenesis. *Traffic (Copenhagen, Denmark)*, 10.1111/tra.12579. https://doi.org/10.1111/tra.12579

Kamangar, F., Dores, G. M., & Anderson, W. F. (2006). Patterns of cancer incidence, mortality, and prevalence across five continents: defining priorities to reduce cancer disparities in different geographic regions of the world. *J Clin Oncol*, *24*(14), 2137-2150. https://doi.org/10.1200/JCO.2005.05.2308

Kim, E., Arnould, T., Sellin, L. K., Benzing, T., Fan, M. J., Grüning, W., . . . Walz, G. (1999). The Polycystic Kidney Disease 1 Gene Product Modulates Wnt Signaling *. *Journal of Biological Chemistry*, *274*(8), 4947-4953. https://doi.org/10.1074/jbc.274.8.4947

Klinkert, K., Rocancourt, M., Houdusse, A., & Echard, A. (2016). Rab35 GTPase couples cell division with initiation of epithelial apico-basal polarity and lumen opening. *Nature Communications*, *7*(1), 11166. https://doi.org/10.1038/ncomms11166

Kotlo, K., Shukla, S., Tawar, U., Skidgel, R. A., & Danziger, R. S. (2007). Aminopeptidase N reduces basolateral Na+-K+-ATPase in proximal tubule cells. *American Journal of Physiology-Renal Physiology*, *293*(4), F1047-F1053.

Kouranti, I., Sachse, M., Arouche, N., Goud, B., & Echard, A. (2006). Rab35 Regulates an Endocytic Recycling Pathway Essential for the Terminal Steps of Cytokinesis. *Current Biology*, *16*(17), 1719-1725. https://doi.org/10.1016/j.cub.2006.07.020

Kroemer, G., & Reed, J. C. (2000). Mitochondrial control of cell death. *Nature medicine*, *6*(5), 513-519.

Kumar, A., Ahmad, A., Vyawahare, A., & Khan, R. (2020). Membrane Trafficking and Subcellular Drug Targeting Pathways [10.3389/fphar.2020.00629]. *Frontiers in Pharmacology*, *11*, 629.

Kuwano, K. (2007). Epithelial cell apoptosis and lung remodeling. *Cell Mol Immunol*, *4*(6), 419-429.

Lalioti, V., Peiró, R., Pérez-Berlanga, M., Tsuchiya, Y., Muñoz, A., Villalba, T., . . . Sandoval, I. V. (2016). Basolateral sorting and transcytosis define the Cu+-regulated translocation of ATP7B to the bile canaliculus. *Journal of cell science*, *129*(11), 2190-2201.

Larsson, S., Söderberg-Nauclér, C., & Möller, E. (1998). PRODUCTIVE CYTOMEGALOVIRUS (CMV) INFECTION EXCLUSIVELY IN CD13-POSITIVE PERIPHERAL BLOOD MONONUCLEAR CELLS FROM CMV-INFECTED INDIVIDUALS: Implications for Prevention of CMV Transmission1. *Transplantation*, *65*(3), 411-415.

Lepore, D. M., Martínez-Núñez, L., & Munson, M. (2018). Exposing the elusive exocyst structure. *Trends in biochemical sciences*, *43*(9), 714-725.

Leung, S.-M., Ruiz, W. G., & Apodaca, G. (2000). Sorting of membrane and fluid at the apical pole of polarized Madin-Darby canine kidney cells. *Molecular biology of the cell*, *11*(6), 2131-2150.

Loos, T., Dekeyzer, L., Struyf, S., Schutyser, E., Gijsbers, K., Gouwy, M., . . . Grillet, B. (2006). TLR ligands and cytokines induce CXCR3 ligands in endothelial cells: enhanced CXCL9 in autoimmune arthritis. *Laboratory investigation*, *86*(9), 902-916.

Lutcke, A., Parton, R. G., Murphy, C., Olkkonen, V. M., Dupree, P., Valencia, A., . . . Zerial, M. (1994). Cloning and subcellular localization of novel rab proteins reveals polarized and cell type-specific expression. *Journal of Cell Science*, *107*(12), 3437-3448.

Luton, F., Vergés, M., Vaerman, J.-P., Sudol, M., & Mostov, K. E. (1999). The SRC Family Protein Tyrosine Kinase p62 yes Controls Polymeric IgA Transcytosis In Vivo. *Molecular Cell*, *4*(4), 627-632. https://doi.org/https://doi.org/10.1016/S1097-2765(00)80213-0

Lütcke, A., Jansson, S., Parton, R. G., Chavrier, P., Valencia, A., Huber, L. A., . . . Zerial, M. (1993). Rab17, a novel small GTPase, is specific for epithelial cells and is induced during cell polarization. *The Journal of cell biology*, *121*(3), 553-564.

Macara, I. G., Guyer, R., Richardson, G., Huo, Y., & Ahmed, S. M. (2014). Epithelial homeostasis. *Curr Biol*, *24*(17), R815-825. https://doi.org/10.1016/j.cub.2014.06.068

Martin-Belmonte, F., & Mostov, K. (2008). Regulation of cell polarity during epithelial morphogenesis. *Current Opinion in Cell Biology*, *20*(2), 227-234. https://doi.org/https://doi.org/10.1016/j.ceb.2008.01.001

Matter, K., Hunziker, W., & Mellman, I. (1992). Basolateral sorting of LDL receptor in MDCK cells: the cytoplasmic domain contains two tyrosine-dependent targeting determinants. *Cell*, *71*(5), 741-753.

Matter, K., & Mellman, I. (1994). Mechamisms of cell polarity: sorting and transport in epithelial cells. *Current opinion in cell biology*, *6*(4), 545-554.

McBride, H. M., Rybin, V., Murphy, C., Giner, A., Teasdale, R., & Zerial, M. (1999). Oligomeric Complexes Link Rab5 Effectors with NSF and Drive Membrane Fusion via Interactions between EEA1 and Syntaxin 13. *Cell*, *98*(3), 377-386. https://doi.org/https://doi.org/10.1016/S0092-8674(00)81966-2

Mellman, I. (1996). Endocytosis and molecular sorting. *Annual review of cell and developmental biology*, *12*(1), 575-625.

Mierzwa, B., & Gerlich, D. W. (2014). Cytokinetic abscission: molecular mechanisms and temporal control. *Developmental cell*, *31*(5), 525-538.

Mina-Osorio, P. (2008). The moonlighting enzyme CD13: old and new functions to target. *Trends in molecular medicine*, *14*(8), 361-371. https://doi.org/10.1016/j.molmed.2008.06.003

Mina-Osorio, P., & Ortega, E. (2004). Signal regulators in FcR-mediated activation of leukocytes? *Trends in immunology*, *25*(10), 529-535.

Mina-Osorio, P., Soto-Cruz, I., & Ortega, E. (2007). A role for galectin-3 in CD13-mediated homotypic aggregation of monocytes. *Biochemical and biophysical research communications*, *353*(3), 605-610.

Mina-Osorio, P., Winnicka, B., O'Conor, C., Grant, C. L., Vogel, L. K., Rodriguez-Pinto, D., . . . Shapiro, L. H. (2008). CD13 is a novel mediator of monocytic/endothelial cell adhesion. *Journal of leukocyte biology*, *84*(2), 448-459. https://doi.org/10.1189/jlb.1107802

Mina-Osorio, P., & Ortega, E. (2005). Aminopeptidase N (CD13) functionally interacts with FcγRs in human monocytes. *Journal of leukocyte biology*, *77*(6), 1008-1017.

Mina-Osorio, P., Shapiro, L. H., & Ortega, E. (2006). CD13 in cell adhesion: aminopeptidase N (CD13) mediates homotypic aggregation of monocytic cells. *Journal of leukocyte biology*, *79*(4), 719-730.

Mizuno, S., Takami, K., Daitoku, Y., Tanimoto, Y., Dinh, T. T. H., Mizuno-Iijima, S., . . . Yagami, K.-i. (2015). Peri-implantation lethality in mice carrying megabase-scale deletion on 5qc3. 3 is caused by Exoc1 null mutation. *Scientific reports*, *5*(1), 1-9.

Morgan, R. L., Behbahani-Nejad, N., Endres, J., Amin, M. A., Lepore, N. J., Du, Y., . . . Fox, D. A. (2016). Localization, shedding, regulation and function of aminopeptidase N/CD13 on fibroblast like synoviocytes. *PloS one*, *11*(9), e0162008.

Mosser, D. M. (2003). The many faces of macrophage activation. *Journal of leukocyte biology*, *73*(2), 209-212.

Mostov, K., Apodaca, G., Aroeti, B., & Okamoto, C. (1992). Plasma membrane protein sorting in polarized epithelial cells. *The Journal of Cell Biology*, *116*(3), 577-583.

Mostov, K. E., & Simister, N. E. (1985). Transcytosis. *Cell*, *43*(2 Pt 1), 389-390.

Mostov, K. E., Verges, M., & Altschuler, Y. (2000). Membrane traffic in polarized epithelial cells. *Current Opinion in Cell Biology*, *12*(4), 483-490. https://doi.org/https://doi.org/10.1016/S0955-0674(00)00120-4

Muller, W. A. (2011). Mechanisms of leukocyte transendothelial migration. *Annual Review of Pathology: Mechanisms of Disease*, *6*, 323-344.
Munson, M., & Novick, P. (2006). The exocyst defrocked, a framework of rods revealed. *Nature structural & molecular biology*, *13*(7), 577-581.
Muro, S. (2018). Alterations in cellular processes involving vesicular trafficking and implications in drug delivery. *Biomimetics*, *3*(3), 19.
Müller, T., Hess, M. W., Schiefermeier, N., Pfaller, K., Ebner, H. L., Heinz-Erian, P., . . . Janecke, A. R. (2008). MYO5B mutations cause microvillus inclusion disease and disrupt epithelial cell polarity. *Nature Genetics*, *40*(10), 1163-1165. https://doi.org/10.1038/ng.225
Nefla, M., Sudre, L., Denat, G., Priam, S., Andre-Leroux, G., Berenbaum, F., & Jacques, C. (2015). The pro-inflammatory cytokine 14-3-3ε is a ligand of CD13 in cartilage. *Journal of cell science*, *128*(17), 3250-3262. https://doi.org/10.1242/jcs.169573
Nelms, B., Dalomba, N. F., & Lencer, W. (2017). A targeted RNAi screen identifies factors affecting diverse stages of receptor-mediated transcytosis. *Journal of Cell Biology*, *216*(2), 511-525.
Nelson, W. J., Dickinson, D. J., & Weis, W. I. (2013). Roles of cadherins and catenins in cell-cell adhesion and epithelial cell polarity. *Prog Mol Biol Transl Sci*, *116*, 3-23. https://doi.org/10.1016/B978-0-12-394311-8.00001-7
Nelson, W. J., & Yeaman, C. (2001). Protein trafficking in the exocytic pathway of polarized epithelial cells. *Trends in cell biology*, *11*(12), 483-486.
Nesbitt, S. A., & Horton, M. A. (1997). Trafficking of matrix collagens through bone-resorbing osteoclasts. *Science*, *276*(5310), 266-269.
Nishida-Fukuda, H. (2019). The Exocyst: Dynamic Machine or Static Tethering Complex? [https://doi.org/10.1002/bies.201900056]. *BioEssays*, *41*(8), 1900056. https://doi.org/https://doi.org/10.1002/bies.201900056
Noda, Y., Takeya, R., Ohno, S., Naito, S., Ito, T., & Sumimoto, H. (2001). Human homologues of the Caenorhabditis elegans cell polarity protein PAR6 as an adaptor that links the small GTPases Rac and Cdc42 to atypical protein kinase C [https://doi.org/10.1046/j.1365-2443.2001.00404.x]. *Genes to Cells*, *6*(2), 107-119. https://doi.org/https://doi.org/10.1046/j.1365-2443.2001.00404.x
Nomura, R., Kiyota, A., Suzaki, E., Kataoka, K., Ohe, Y., Miyamoto, K., . . . Fujimoto, T. (2004). Human coronavirus 229E binds to CD13 in rafts and enters the cell through caveolae. *Journal of virology*, *78*(16), 8701-8708.
Novick, P., & Zerial, M. (1997). The diversity of Rab proteins in vesicle transport. *Current Opinion in Cell Biology*, *9*(4), 496-504. https://doi.org/https://doi.org/10.1016/S0955-0674(97)80025-7
Okutani, D., Lodyga, M., Han, B., & Liu, M. (2006). Src protein tyrosine kinase family and acute inflammatory responses. *American Journal of Physiology-Lung Cellular and Molecular Physiology*, *291*(2), L129-L141.
Oztan, A., Silvis, M., Weisz, O. A., Bradbury, N. A., Hsu, S.-C., Goldenring, J. R., . . . Apodaca, G. (2007). Exocyst requirement for endocytic traffic directed toward the apical and basolateral poles of polarized MDCK cells. *Molecular biology of the cell*, *18*(10), 3978-3992.

Pasqualini, R., Koivunen, E., Kain, R., Lahdenranta, J., Sakamoto, M., Stryhn, A., . . . Ruoslahti, E. (2000). Aminopeptidase N is a receptor for tumor-homing peptides and a target for inhibiting angiogenesis. *Cancer research*, *60*(3), 722-727.

Perez Bay, A. E., Schreiner, R., Mazzoni, F., Carvajal-Gonzalez, J. M., Gravotta, D., Perret, E., . . . Rodriguez-Boulan, E. J. (2013). The kinesin KIF16B mediates apical transcytosis of transferrin receptor in AP-1B-deficient epithelia. *The EMBO journal*, *32*(15), 2125-2139.

Perou, C. M., Sørlie, T., Eisen, M. B., Van De Rijn, M., Jeffrey, S. S., Rees, C. A., . . . Akslen, L. A. (2000). Molecular portraits of human breast tumours. *nature*, *406*(6797), 747-752.

Pocha, Shirin M., & Knust, E. (2013). Complexities of Crumbs Function and Regulation in Tissue Morphogenesis. *Current Biology*, *23*(7), R289-R293. https://doi.org/https://doi.org/10.1016/j.cub.2013.03.001

Polyak, K. (2007). Breast cancer: origins and evolution. *The Journal of clinical investigation*, *117*(11), 3155-3163. https://doi.org/10.1172/JCI33295

Priam, S., Bougault, C., Houard, X., Gosset, M., Salvat, C., Berenbaum, F., & Jacques, C. (2013). Identification of Soluble 14-3-3∈ as a Novel Subchondral Bone Mediator Involved in Cartilage Degradation in Osteoarthritis [https://doi.org/10.1002/art.37951]. *Arthritis & Rheumatism*, *65*(7), 1831-1842. https://doi.org/https://doi.org/10.1002/art.37951

Proost, P., Mortier, A., Loos, T., Vandercappellen, J., Gouwy, M., Ronsse, I., . . . Van Damme, J. (2007). Proteolytic processing of CXCL11 by CD13/aminopeptidase N impairs CXCR3 and CXCR7 binding and signaling and reduces lymphocyte and endothelial cell migration. *Blood*, *110*(1), 37-44. https://doi.org/10.1182/blood-2006-10-049072

Rausch, D. M., Lewis, D. L., Barker, J. L., & Eiden, L. E. (1990). Functional expression of dihydropyridine-insensitive calcium channels during PC12 cell differentiation by nerve growth factor (NGF), oncogenic ras, or src tyrosine kinase. *Cellular and molecular neurobiology*, *10*(2), 237-255.

Rejon, C., Al-Masri, M., & McCaffrey, L. (2016). Cell Polarity Proteins in Breast Cancer Progression [https://doi.org/10.1002/jcb.25553]. *Journal of Cellular Biochemistry*, *117*(10), 2215-2223. https://doi.org/https://doi.org/10.1002/jcb.25553

Rivera-Molina, F., & Toomre, D. (2013). Live-cell imaging of exocyst links its spatiotemporal dynamics to various stages of vesicle fusion. *Journal of Cell Biology*, *201*(5), 673-680.

Rodriguez-Boulan, E., & Macara, I. G. (2014). Organization and execution of the epithelial polarity programme. *Nat Rev Mol Cell Biol*, *15*(4), 225-242. https://doi.org/10.1038/nrm3775

Roeth, J. F., Sawyer, J. K., Wilner, D. A., & Peifer, M. (2009). Rab11 Helps Maintain Apical Crumbs and Adherens Junctions in the Drosophila Embryonic Ectoderm. *PLOS ONE*, *4*(10), e7634. https://doi.org/10.1371/journal.pone.0007634

Roignot, J., Peng, X., & Mostov, K. (2013). Polarity in mammalian epithelial morphogenesis. *Cold Spring Harb Perspect Biol*, *5*(2). https://doi.org/10.1101/cshperspect.a013789

Roland, J. T., Kenworthy, A. K., Peranen, J., Caplan, S., & Goldenring, J. R. (2007). Myosin Vb interacts with Rab8a on a tubular network containing EHD1 and EHD3. *Molecular biology of the cell*, *18*(8), 2828-2837.

Rosado, J. A., Graves, D., & Sage, S. O. (2000). Tyrosine kinases activate store-mediated Ca2+ entry in human platelets through the reorganization of the actin cytoskeleton. *Biochemical Journal*, *351*(2), 429-437.

Rowe, S. M., Miller, S., & Sorscher, E. J. (2005). Cystic Fibrosis. *New England Journal of Medicine*, *352*(19), 1992-2001. https://doi.org/10.1056/NEJMra043184

Saitoh, S., Maruyama, T., Yako, Y., Kajita, M., Fujioka, Y., Ohba, Y., . . . Fujita, Y. (2017). Rab5-regulated endocytosis plays a crucial role in apical extrusion of transformed cells. *Proceedings of the National Academy of Sciences*, *114*(12), E2327. https://doi.org/10.1073/pnas.1602349114

Santos, A. N., Langner, J., & Riemann, D. (2002). Enzymatic activity is not a precondition for the intracellular calcium increase mediated by mAbs specific for aminopeptidase N/CD13. In *Cellular Peptidases in Immune Functions and Diseases 2* (pp. 43-47). Springer.

Sato, T., Mushiake, S., Kato, Y., Sato, K., Sato, M., Takeda, N., . . . Tsuji, A. (2007). The Rab8 GTPase regulates apical protein localization in intestinal cells. *Nature*, *448*(7151), 366-369.

Schaefer, A. W., Kamei, Y., Kamiguchi, H., Wong, E. V., Rapoport, I., Kirchhausen, T., . . . Lemmon, V. (2002). L1 endocytosis is controlled by a phosphorylation-dephosphorylation cycle stimulated by outside-in signaling by L1. *The Journal of cell biology*, *157*(7), 1223-1232.

Schaerer, E., Neutra, M. R., & Kraehenbuhl, J.-P. (1991). Molecular and cellular mechanisms involved in transepithelial transport. *The Journal of membrane biology*, *123*(2), 93-103.

Scheiffele, P., Peränen, J., & Simons, K. (1995). N-glycans as apical sorting signals in epithelial cells. *Nature*, *378*(6552), 96-98.

Schimmöller, F., Simon, I., & Pfeffer, S. R. (1998). Rab GTPases, directors of vesicle docking. *Journal of Biological Chemistry*, *273*(35), 22161-22164.

Schlüter, M. A., Pfarr, C. S., Pieczynski, J., Whiteman, E. L., Hurd, T. W., Fan, S., . . . Margolis, B. (2009). Trafficking of Crumbs3 during cytokinesis is crucial for lumen formation. *Molecular biology of the cell*, *20*(22), 4652-4663. https://doi.org/10.1091/mbc.e09-02-0137

Schneeberger, K., Roth, S., Nieuwenhuis, E. E. S., & Middendorp, S. (2018). Intestinal epithelial cell polarity defects in disease: lessons from microvillus inclusion disease. *Disease Models & Mechanisms*, *11*(2), dmm031088. https://doi.org/10.1242/dmm.031088

Schnitzer, J. E., Carley, W. W., & Palade, G. E. (1988). Albumin interacts specifically with a 60-kDa microvascular endothelial glycoprotein. *Proceedings of the National Academy of Sciences*, *85*(18), 6773-6777.

Schnitzer, J. E., Oh, P., Pinney, E., & Allard, J. (1994). Filipin-sensitive caveolae-mediated transport in endothelium: reduced transcytosis, scavenger endocytosis, and capillary permeability of select macromolecules. *The Journal of cell biology*, *127*(5), 1217-1232.

Shajahan, A. N., Timblin, B. K., Sandoval, R., Tiruppathi, C., Malik, A. B., & Minshall, R. D. (2004). Role of Src-induced dynamin-2 phosphorylation in caveolae-mediated endocytosis in endothelial cells. *Journal of Biological Chemistry*, *279*(19), 20392-20400.

Sharma, G. N., Dave, R., Sanadya, J., Sharma, P., & Sharma, K. K. (2010). Various types and management of breast cancer: an overview. *Journal of advanced pharmaceutical technology & research*, *1*(2), 109-126.

Sharma, N., Low, S. H., Misra, S., Pallavi, B., & Weimbs, T. (2006). Apical targeting of syntaxin 3 is essential for epithelial cell polarity. *Journal of cell biology*, *173*(6), 937-948.

Shi, C., & Pamer, E. G. (2011). Monocyte recruitment during infection and inflammation. *Nature reviews immunology*, *11*(11), 762-774.
Shipp, M. A., & Look, A. T. (1993). Hematopoietic differentiation antigens that are membrane-associated enzymes: cutting is the key!
Simonsen, A., Lippe, R., Christoforidis, S., Gaullier, J.-M., Brech, A., Callaghan, J., . . . Stenmark, H. (1998). EEA1 links PI (3) K function to Rab5 regulation of endosome fusion. *Nature*, *394*(6692), 494-498.
Siziopikou, K. P. (2013). Ductal carcinoma in situ of the breast: current concepts and future directions. *Archives of pathology & laboratory medicine*, *137*(4), 462-466.
Skop, A. R., Liu, H., Yates, J., Meyer, B. J., & Heald, R. (2004). Dissection of the mammalian midbody proteome reveals conserved cytokinesis mechanisms. *Science*, *305*(5680), 61-66.
Song, W., Bomsel, M., Casanova, J., Vaerman, J. P., & Mostov, K. (1994). Stimulation of transcytosis of the polymeric immunoglobulin receptor by dimeric IgA. *Proceedings of the National Academy of Sciences of the United States of America*, *91*(1), 163-166. https://doi.org/10.1073/pnas.91.1.163
Stein, M.-P., Wandinger-Ness, A., & Roitbak, T. (2002). Altered trafficking and epithelial cell polarity in disease. *Trends in Cell Biology*, *12*(8), 374-381. https://doi.org/https://doi.org/10.1016/S0962-8924(02)02331-0
Stenmark, H. (2009). Rab GTPases as coordinators of vesicle traffic. *Nature Reviews Molecular Cell Biology*, *10*(8), 513-525. https://doi.org/10.1038/nrm2728
Subramani, J., Ghosh, M., Rahman, M. M., Caromile, L. A., Gerber, C., Rezaul, K., . . . Shapiro, L. H. (2013). Tyrosine phosphorylation of CD13 regulates inflammatory cell-cell adhesion and monocyte trafficking. *Journal of immunology (Baltimore, Md. : 1950)*, *191*(7), 3905-3912. https://doi.org/10.4049/jimmunol.1301348
Sørlie, T., Perou, C. M., Tibshirani, R., Aas, T., Geisler, S., Johnsen, H., . . . Jeffrey, S. S. (2001). Gene expression patterns of breast carcinomas distinguish tumor subclasses with clinical implications. *Proceedings of the National Academy of Sciences*, *98*(19), 10869-10874.
Tsukita, S., Furuse, M., & Itoh, M. (2001). Multifunctional strands in tight junctions. *Nature reviews Molecular cell biology*, *2*(4), 285-293.
Tuma, P. L., & Hubbard, A. L. (2003). Transcytosis: Crossing Cellular Barriers. *Physiological Reviews*, *83*(3), 871-932. https://doi.org/10.1152/physrev.00001.2003
Tuvia, S., Garver, T. D., & Bennett, V. (1997). The phosphorylation state of the FIGQY tyrosine of neurofascin determines ankyrin-binding activity and patterns of cell segregation. *Proceedings of the National Academy of Sciences*, *94*(24), 12957-12962.
van der Sluijs, P., Hull, M., Webster, P., Mâle, P., Goud, B., & Mellman, I. (1992). The small GTP-binding protein rab4 controls an early sorting event on the endocytic pathway. *Cell*, *70*(5), 729-740.
van Ijzendoorn, S. C. D., Tuvim, M. J., Weimbs, T., Dickey, B. F., & Mostov, K. E. (2002). Direct interaction between Rab3b and the polymeric immunoglobulin receptor controls ligand-stimulated transcytosis in epithelial cells. *Developmental cell*, *2*(2), 219-228.
Van Itallie, C. M., & Anderson, J. M. (2014). Architecture of tight junctions and principles of molecular composition. *Seminars in cell & developmental biology*, *36*, 157-165. https://doi.org/10.1016/j.semcdb.2014.08.011

Walsh, F. S., & Doherty, P. (1997). Neural cell adhesion molecules of the immunoglobulin superfamily: role in axon growth and guidance. *Annual review of cell and developmental biology*, *13*(1), 425-456.

Wang, E., Brown, P. S., Aroeti, B., Chapin, S. J., Mostov, K. E., & Dunn, K. W. (2000). Apical and basolateral endocytic pathways of MDCK cells meet in acidic common endosomes distinct from a nearly-neutral apical recycling endosome. *Traffic*, *1*(6), 480-493.

Wang, L.-T., Rajah, A., Brown, C. M., & McCaffrey, L. (2021). CD13 orients the apical-basal polarity axis necessary for lumen formation. *Nature Communications*, *12*(1), 4697. https://doi.org/10.1038/s41467-021-24993-x

Wang, S., & Hsu, S.-C. (2006). The molecular mechanisms of the mammalian exocyst complex in exocytosis. In: Portland Press Ltd.

Wang, X., Kumar, R., Navarre, J., Casanova, J. E., & Goldenring, J. R. (2000). Regulation of vesicle trafficking in madin-darby canine kidney cells by Rab11a and Rab25. *Journal of Biological Chemistry*, *275*(37), 29138-29146.

Watson, P., Jones, A. T., & Stephens, D. J. (2005). Intracellular trafficking pathways and drug delivery: fluorescence imaging of living and fixed cells. *Advanced drug delivery reviews*, *57*(1), 43-61.

Wentworth, D. E., & Holmes, K. V. (2001). Molecular determinants of species specificity in the coronavirus receptor aminopeptidase N (CD13): influence of N-linked glycosylation. *Journal of virology*, *75*(20), 9741-9752. https://doi.org/10.1128/JVI.75.20.9741-9752.2001

Wiegerinck, C. L., Janecke, A. R., Schneeberger, K., Vogel, G. F., van Haaften–Visser, D. Y., Escher, J. C., . . . Middendorp, S. (2014). Loss of Syntaxin 3 Causes Variant Microvillus Inclusion Disease. *Gastroenterology*, *147*(1), 65-68.e10. https://doi.org/10.1053/j.gastro.2014.04.002

Wilson, J. M., de Hoop, M., Zorzi, N., Toh, B. H., Dotti, C. G., & Parton, R. G. (2000). EEA1, a tethering protein of the early sorting endosome, shows a polarized distribution in hippocampal neurons, epithelial cells, and fibroblasts. *Molecular biology of the cell*, *11*(8), 2657-2671. https://doi.org/10.1091/mbc.11.8.2657

Wilson, P. D. (1997). Epithelial cell polarity and disease. *American Journal of Physiology-Renal Physiology*, *272*(4), F434-F442.

Wilson, P. D. (2011). Apico-basal polarity in polycystic kidney disease epithelia. *Biochimica et Biophysica Acta (BBA) - Molecular Basis of Disease*, *1812*(10), 1239-1248. https://doi.org/https://doi.org/10.1016/j.bbadis.2011.05.008

Wilson, P. D., Sherwood, A. C., Palla, K., Du, J., Watson, R., & Norman, J. T. (1991). Reversed polarity of Na(+) -K(+) -ATPase: mislocation to apical plasma membranes in polycystic kidney disease epithelia. *American Journal of Physiology-Renal Physiology*, *260*(3), F420-F430. https://doi.org/10.1152/ajprenal.1991.260.3.F420

Witkowska, A., Heinz, L. P., Grubmüller, H., & Jahn, R. (2021). Tight docking of membranes before fusion represents a metastable state with unique properties. *Nature Communications*, *12*(1), 1-7.

Wong, A. H. M., Zhou, D., & Rini, J. M. (2012). The X-ray crystal structure of human aminopeptidase N reveals a novel dimer and the basis for peptide processing. *The Journal of biological chemistry*, *287*(44), 36804-36813. https://doi.org/10.1074/jbc.M112.398842

Wu, B., & Guo, W. (2015). The exocyst at a glance. *Journal of cell science*, *128*(16), 2957-2964.

Yamanaka, T., & Ohno, S. (2008). Role of Lgl/Dlg/Scribble in the regulation of epithelial junction, polarity and growth. *Frontiers in Bioscience-Landmark*, *13*(17), 6693-6707.
Yeager, C. L., Ashmun, R. A., Williams, R. K., Cardellichio, C. B., Shapiro, L. H., Look, A. T., & Holmes, K. V. (1992). Human aminopeptidase N is a receptor for human coronavirus 229E. *Nature*, *357*(6377), 420-422. https://doi.org/10.1038/357420a0
Yeaman, C., Grindstaff, K. K., & Nelson, W. J. (1999). New perspectives on mechanisms involved in generating epithelial cell polarity. *Physiological reviews*, *79*(1), 73-98.
Yeaman, C., Grindstaff, K. K., Wright, J. R., & Nelson, W. J. (2001). Sec6/8 complexes on trans-Golgi network and plasma membrane regulate late stages of exocytosis in mammalian cells. *The Journal of cell biology*, *155*(4), 593-604.
Yue, P., Zhang, Y., Mei, K., Wang, S., Lesigang, J., Zhu, Y., . . . Guo, W. (2017). Sec3 promotes the initial binary t-SNARE complex assembly and membrane fusion. *Nature communications*, *8*(1), 1-12.
Zacchi, P., Stenmark, H., Parton, R. G., Orioli, D., Lim, F., Giner, A., . . . Murphy, C. (1998). Rab17 regulates membrane trafficking through apical recycling endosomes in polarized epithelial cells. *The Journal of cell biology*, *140*(5), 1039-1053.
Zhan, L., Rosenberg, A., Bergami, K. C., Yu, M., Xuan, Z., Jaffe, A. B., . . . Muthuswamy, S. K. (2008). Deregulation of scribble promotes mammary tumorigenesis and reveals a role for cell polarity in carcinoma. *Cell*, *135*(5), 865-878.
Zhang, X.-M., Ellis, S., Sriratana, A., Mitchell, C. A., & Rowe, T. (2004). Sec15 is an effector for the Rab11 GTPase in mammalian cells. *Journal of Biological Chemistry*, *279*(41), 43027-43034.
Zhao, B., Li, L., Lei, Q., & Guan, K.-L. (2010). The Hippo-YAP pathway in organ size control and tumorigenesis: an updated version. *Genes & development*, *24*(9), 862-874. https://doi.org/10.1101/gad.1909210
Zhao, B., Li, L., Lu, Q., Wang, L. H., Liu, C.-Y., Lei, Q., & Guan, K.-L. (2011). Angiomotin is a novel Hippo pathway component that inhibits YAP oncoprotein. *Genes & development*, *25*(1), 51-63. https://doi.org/10.1101/gad.2000111
Zhu, W., Saddar, S., Seetharam, D., Chambliss, K. L., Longoria, C., Silver, D. L., . . . Mineo, C. (2008). The scavenger receptor class B type I adaptor protein PDZK1 maintains endothelial monolayer integrity. *Circulation research*, *102*(4), 480-487.